Zoologica Scripta

Molecular and morphological phylogeny of Diplazontinae (Hymenoptera, Ichneumonidae)

Seraina Klopfstein, Donald L. J. Quicke, Christian Kropf & Holger Frick

Submitted: 22 September 2010
Accepted: 5 May 2011
doi:10.1111/j.1463-6409.2011.00481.x

Klopfstein, S., Quicke, D. L. J., Kropf, C. & Frick, H. (2011) Molecular and morphological phylogeny of Diplazontinae (Hymenoptera, Ichneumonidae). — *Zoologica Scripta*, *40*, 379–402.

Parasitoid wasps are among the most species rich and at the same time most understudied of all metazoan taxa. To understand their diversification and test hypotheses about their evolution, we need robust phylogenetic hypotheses. Here, we reconstruct the phylogeny of the subfamily Diplazontinae using four genes and 66 morphological characters both in separate analyses and in a total evidence approach. The resulting phylogeny is highly resolved, with most clades supported by multiple independent data partitions. It contains three highly supported genus groups, for which we suggest morphological and behavioural synapomorphies. The placement of some of the genera, especially *Xestopelta* Dasch, is unexpected, but also supported by morphology. Most of the genera are retrieved as monophyletic, with the exception of the morphologically diverse genus *Syrphoctonus* Förster. We split this genus into three genera, including *Fossatyloides* gen. n., to restore the phylogeny–classification link. Conflict between the morphological and the molecular topology was mostly resolved in favour of the molecular partition in the total evidence approach. We discuss reasons for this finding, and suggest strategies for future taxon and character sampling in Diplazontinae.

Corresponding author: *Seraina Klopfstein, Naturhistoriska Riksmuseet, Enheten för Entomologi, Box 50007, 104 05 Stockholm, Sweden. E-mail: seraina.klopfstein@nrm.se*

Seraina Klopfstein, Christian Kropf and Holger Frick, Natural History Museum (Invertebrates), Bernastrasse 15, CH-3005 Bern, Switzerland. E-mails: christian.kropf@nmbe.ch, holger.frick@gmx.li

Seraina Klopfstein and Holger Frick, Division of Community Ecology, Institute of Ecology and Evolution, University of Bern, Baltzerstr. 7, 3012 Bern, Switzerland

Donald L. J. Quicke, Division of Biology, Imperial College London, Silwood Park Campus, Ascot, Berkshire SL5 7PY, UK; Department of Entomology, Natural History Museum, London SW7 5BD, UK. E-mail: d.quicke@imperial.ac.uk

Introduction

The subfamily Diplazontinae represents one of the smaller, morphologically more homogeneous subfamilies of the species-rich Ichneumonidae. As far as we are aware, these parasitoids are associated exclusively with hoverfly hosts (Diptera, Syrphidae), with a strong bias towards the aphidophagous species (Kamal 1926; Dusek *et al.* 1979; Rotheray 1981, 1984, 1990; Fitton & Rotheray 1982; Ngamo Tinkeu & Hance 1997). Their association with a closely related group of hosts makes them an ideal group to study the evolution of host relations and specialization (Page & Charleston 1998). Moreover, a peculiar mode of antennal courtship has recently been reported from a species of this group (Steiner *et al.* 2010). To study the evolution of such ecological or behavioural characters, robust phylogenetic hypotheses of the group are needed. In Diplazontinae, both taxonomy and phylogeny have, to date, only received limited attention, as is the case in most parasitoid groups (Quicke 1997; Jones *et al.* 2009). The only fauna for which Diplazontinae have been thoroughly revised is the Nearctic (Dasch 1964), and this morphological revision did not include any phylogenetic analysis, but only some informal comments about relationships between genera. Intra-generic relationships were also proposed by Fitton & Rotheray (1982), but these authors usually did not present synapomorphies for the suggested groupings. The only previous phylogenetic analysis of the subfamily with reasonable generic coverage included 42 species and was based on two molecular markers (Klopfstein *et al.* 2010a). It found three highly supported genus groups which were informally called *Sussaba*, *Syrphoctonus* and *Diplazon* genus groups. The placement of some genera in these groups was unexpected, for example, the highly derived *Bioblapsis* in the *Syrphoctonus* genus group and *Campocraspedon* in the *Diplazon* genus

group. Two genera, *Syrphoctonus* Förster and *Tymmophorus* Schmiedeknecht, were recovered as paraphyletic, with varying support. We here extend this study by including 66 morphological characters and two additional molecular markers, the mitochondrial NADH1 and the F2 copy of the nuclear elongation factor 1α (EF1α). The parallel use of molecular and morphological data allows us to obtain and test morphological synapomorphies of higher level taxa and provides a basis for exploring congruence and conflict among these different sources of data (Patterson *et al.* 1993; Carpenter & Wheeler 1999; Wahlberg *et al.* 2005). Using congruence with the independently derived molecular dataset as a measure of performance (Miyamoto & Fitch 1995; Cunningham 1997), we identify the preferred weighting strategy and strength for the morphological data partition when analysed under the parsimony criterion. The extended taxon sampling now including 70 species and two additional genera allows us to test the previous phylogenetic hypothesis and to assess the status of the unsupported genera. Additionally, we include two genera which in the past have been difficult to associate with other genera, that is, *Xestopelta* Dasch and *Schachticraspedon* Diller.

Materials and methods

Taxon sampling

We included 85 individuals of 70 Diplazontinae species (73 species for the molecular dataset) in our study, covering 13 of the 20 described genera (Appendix 1). Only species for which we could obtain sequences from all four molecular markers were included in the analyses, although for six species [*Promethes sulcator* (Gravenhorst), *Sussaba dorsalis* (Holmgren), *Sussaba flavipes* (Lucas), *Sussaba pulchella* (Holmgren), *Syrphoctonus fissorius* (Gravenhorst) and *Woldstedtius flavolineatus* (Gravenhorst)], different specimens had to be used to obtain sequences from the different genes. To provide as much information as possible, for some undescribed taxa, we use names that are not yet available; these are disclaimed from nomenclatural purposes according to article 8.3 of the International Code of Zoological Nomenclature (1999). These new names are *Diplazon wymanni*, *Diplazon zetteli*, *Homotropus lucidus*, *Schachticraspedon kropfi*, *Sussaba roberti* and *Woldstedtius bauri*.

Monophyly of the Diplazontinae is supported by a number of adult (Beirne 1941; Dasch 1964; Townes 1971; Wahl 1990; Wahl & Gauld 1998), larval (Wahl 1990; Wahl & Gauld 1998) and biological characters (e.g. Dasch 1964; Fitton & Rotheray 1982; Yu *et al.* 2005) and in molecular studies (Quicke *et al.* 2009). They form part of the informal subfamilial clade 'Pimpliformes'. As the relationships among most pimpliform subfamilies are not convincingly resolved (Quicke *et al.* 2009), we included six representatives from five pimpline subfamilies together with a member of the related Ichneumoniformes; the latter was used as the functional outgroup for the whole dataset (Appendix 1).

Morphological characters for phylogenetic reconstruction

As there is currently no morphological phylogeny of the group available, we newly scored 66 characters for most of the species included in the molecular analysis (Appendix 2). This number might seem low compared with the number of species analysed, but reflects the fact that we used a dense taxon sampling at the species level, and that the Diplazontinae are comparatively uniform in terms of discrete morphological differences. Many closely related species only show small morphological differences, which often involve only colour or sculpture characters, which amount to 11 and 12 of the 66 characters, respectively. To reduce any bias that could stem from excluding characters that are considered unreliable at higher taxonomic levels, we aimed to include every character that was parsimony informative and different between any two species and that could be scored unambiguously. The matrix contains both new characters (characters 3, 6, 7, 8, 32, 38, 44, 45, 47, 52, 53, 54, 55, 56, 61, 62; see Appendix 2) and characters mentioned in taxonomic revisions or keys of the group (Beirne 1941; Dasch 1964; Townes 1971; Fitton & Rotheray 1982). Some character states are illustrated in Fig. 1. The ninth sternite and ninth and tenth tergites of the male have been studied in Diplazontinae by Beirne (1941) and Dasch (1964), who both mainly used them for species delimitation. This character complex proved to be of great value for defining genus groups in the present study. The different states of this character complex are shown in Fig. 2. Descriptions of characters, their states and consistency index (CI) and retention index (RI) on the total evidence topology are shown in Appendix 2, and the character matrix is provided as Supporting information. Unless mentioned otherwise, the characters were scored based on female specimens. Morphological terminology follows Townes (1969).

Molecular methods

Genomic DNA was extracted from whole specimens preserved in 80% ethanol and from dried specimens using the Promega Wizard (Promega UK, Southampton, United Kingdom) kit for blood and tissue extractions. Vouchers and DNA samples are kept at the Natural History Museum in Berne, at the Swedish Malaise Trap Project and in the Insect Museum of the University of Wyoming (Appendix 1). Approximately 700 bp from the 5′ end of the mitochondrial cytochrome oxidase I (CO1) gene were amplified using the primers designed by Folmer *et al.* (1994) (LCO 5′-GGT CAA CAA ATC ATA AAG ATA TTG G-3′, HCO 5′-TAA ACT TCA GGG TGA CCA

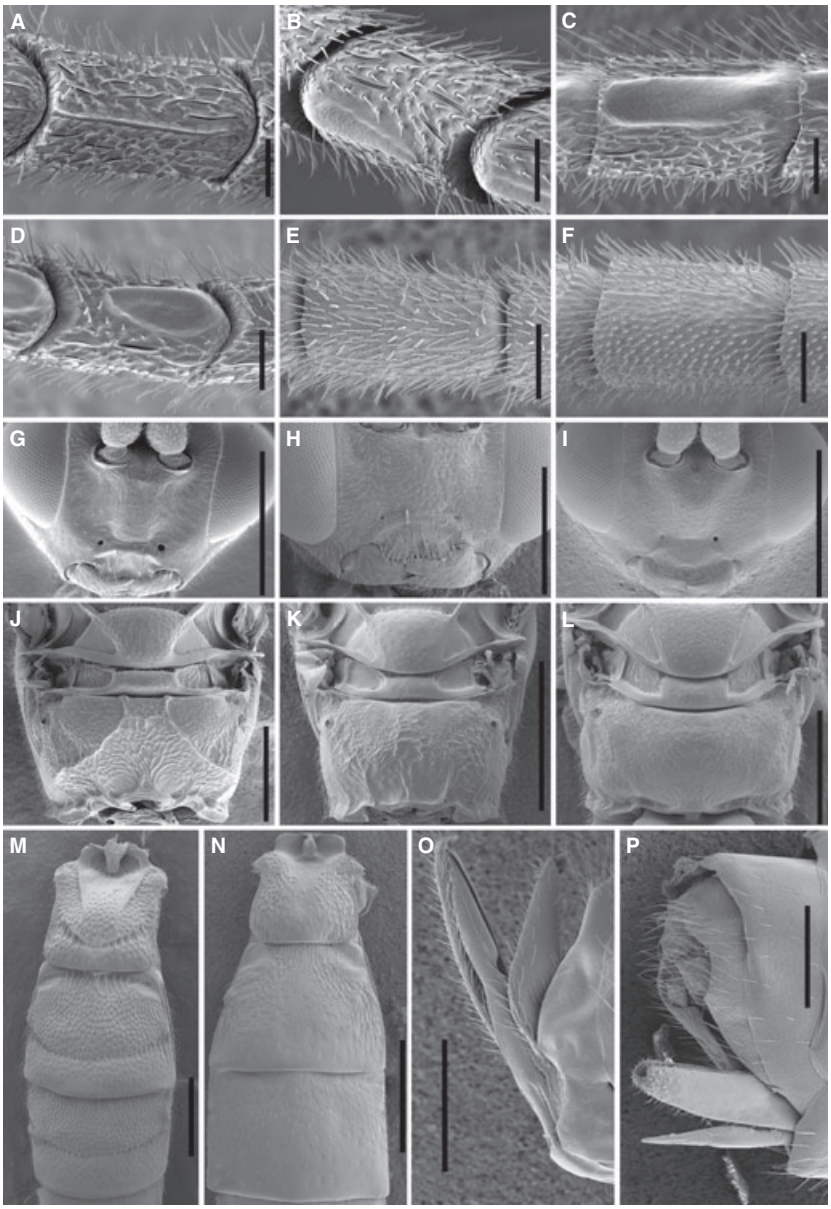

Fig. 1 Some of the morphological characters used in the phylogenetic analysis. A–D. Tyloids on the antennae of male diplazontines. —A. Linear, narrow tyloid in *Syrphoctonus tarsatorius*. —B. Drop-shaped tyloid in *Sussaba erigator*. —C. Linear, broad tyloid in *Enizemum ornatum*. —D. Oval, broad tyloid in *Sussaba pulchella*. E–F. Ventral surface of antenna in female Diplazontinae. —E. Unmodified ventral surface bearing multiporous plate sensillae in *Homotropus signatus*. —F. Modified ventral surface in *Homotropus crassicrus* with short cone-like sensillae and multiporous plate sensillae present only on dorsal surface. G–I. Faces and clypei. —G. *Sussaba flavipes* with vertical depressions arising from tentorial pits, and with clypeus with basal elevation rendering the remainder concave. —H. *Diplazon scutatorius* without vertical depressions, clypeus with a basal elevation. —I. *Homotropus signatus* without vertical depressions, clypeus apically impressed which renders the basal part convex. J–L. Propodeum showing carination. —J. Full set of carinae on the propodeum of *Diplazon scutatorius*. —K. Carinae partly reduced, only weakly indicating areas in *Homotropus signatus*. —L. Carinae completely reduced in *Woldstedtius holarcticus*. M–N. Sculpture on metasomal segments 1–3. —M. Tergites with transverse impressions and strong punctures in *Diplazon scutatorius*. —N. Tergites without impressions and mainly coriaceous sculpture in *Homotropus crassicrus*. O–P. Ovipositor sheats. —O. Ovipositor shown enclosed by one sheat which is closed at the tip in *Sussaba aciculata*. —P. Ovipositor sheat diagonally truncate in *Homotropus signatus*. Scale bars indicate 50 μm (A–F), 500 μm (G–N), and 200 μm (O–P), respectively.

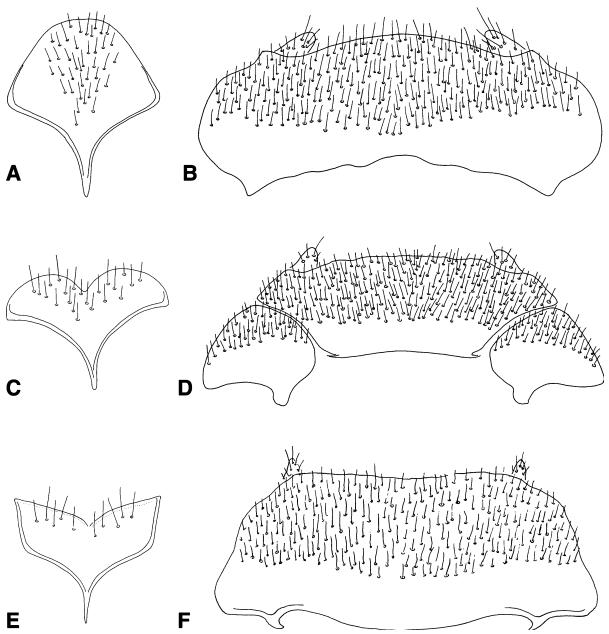

Fig. 2 Ninth sternites (A, C, E) and ninth and tenth tergites (B, D, F) of male Diplazontinae. —A–B. Unilobate ninth sternite and fused ninth and tenth tergites in *Sussaba erigator*. —C–D. Bilobate ninth sternite and separate ninth and tenth tergites in *Homotropus nigritarsus*. —E–F. Bilobate ninth sternite with acute outer angles and fused ninth and tenth tergites in *Daschia brevitarsis*. The figures are not in scale.

AAA AAT CA-3′). To obtain about 480 bp of the second mitochondrial gene, NADH dehydrogenase 1 (ND1), we first used primers as published in the literature, which we then elongated according to the obtained sequences by 1 and 6 bp, respectively, to improve amplification in more difficult specimens (Smith *et al.* 1999; elongations in square brackets, fwd: 5′-ACT AAT TCA GAT TCT CCT TCT [G]-3′, rev: 5′-CAA CCT TTT AGT GAT GC [T ATT AA]-3′). For the nuclear 28S rRNA, we obtained approximately 700 bp of the D2 and partial D3 region using the primers designed by Belshaw & Quicke (1997) (fwd: 5′-A AGA GAG AGT TCA AGA GTA CGT G-3′) and Mardulyn & Whitfield (1999) (rev: 5′-TAG TTC ACC ATC TTT CGG GTC CC-3′). To amplify the second copy of EF1α (F2 copy), we used the forward primer by Belshaw & Quicke (1997) (fwd: 5′-AG ATG GGY AAR GGT TCC TTC AA-3′) and a reverse primer compiled for this study (rev: 5′-G CAG GGG AAG ACG AAG AGC C-3′), which together amplified about 600 bp of exon 2. To make sure that we had only F2 copy sequences in our matrix (Danforth & Ji 1998), we compared our sequences with an unpublished matrix from the HymAToL project containing both the F1 and the F2 copy from various hymenopteran species.

Polymerase chain reactions (PCR) were carried out in 20 μL final volumes using Promega GoTaq Flexi DNA Polymerase kits. Final volumes contained 30 pmol $MgCl_2$, 16 pmol of both primers, 4 pmol of each dNTP, 0.3 U Taq polymerase and 2 μL genomic DNA. PCR conditions were: 94 °C for 2 min, 35 cycles of 30 s at 94 °C, 30 s at the respective annealing temperature (51 °C for CO1, 48 °C for ND1, 53 °C for 28S and 57 °C for EF1α) and 1 min at 72 °C, followed by a final extension at 72 °C for 10 min. PCR products were either purified using the GFXTM DNA and Gel Purification kit (Amersham Biosciences, Little Chalfont, UK) or by the purification service of Macrogen Korea. The PCR products were sequenced on an ABI 377 automated sequencer using Big Dye Terminator technology (Applied Biosystems, Warrington, UK). Sixty of the 90 28S sequences and 59 of the CO1 sequences and all the ND1 and EF1α data were newly generated for this study; the remainder were taken from Klopfstein *et al.* (2010a). All sequences have been deposited in the GenBank database, the new sequences under accession nos. GU597538–GU597836 (Appendix 1).

The sequences of the three protein-coding genes (CO1, ND1 and EF1α) were aligned using the MAFFT program (Katoh *et al.* 2009) as available from the web server (http://mafft.cbrc.jp/alignment/server/) with automatic choice of alignment strategy and default parameters. Except for one 3-bp gap in the four *Promethes* species in ND1, no indels were detected. The D2–D3 region of the large subunit of 28S rRNA was aligned according to published secondary structure maps of ichneumonids (Gillespie *et al.* 2005), identifying the stem regions for partitioning and the pairing nucleotide positions for the application of the doublet model in MrBayes (http://mrbayes.csit.fsu.edu) (see below). Of the regions of ambiguous alignment as identified by Gillespie *et al.* (2005), only those that were length-conserved across the alignment were included in the analyses, while length-variable stretches were excluded. The excluded regions together made up for 68 bp of originally 636 bp [region of ambiguous alignment (RAA) 2, 9 bp; non-homologous region (NHR) 2, 21 bp; RAA 15, 17 bp; RAA 19, 21 bp]. All gap positions were excluded from subsequent analyses. Alignments can be downloaded from TreeBASE (http://purl.org/phylo/treebase/phylows/study/TB2:S11589) and a file including secondary structure annotations of 28S can be obtained from SK on request.

Analyses of morphological data

Morphological data was analysed both separately and combined with the molecular data (total evidence approach, see below). For the separate analyses under parsimony, we first applied traditional searches with tree-bisection-reconnec-

tion (TBR) as implemented in the program TNT (Goloboff *et al.* 2008), using 1000 replicates each holding 10 trees. The low number of hits (13.8%, in the case of equal weights, up to 70% for implied weighting, see below) indicated that the tree space might not have been searched effectively enough. Therefore, we broadened the tree search using different combinations of the number of replicates and trees held, ranging from 10/10 000 to 10 000/10, and repeated all searches using a TBR-ratchet with 200 iterations. The shortest trees found did not differ in length from the analyses using TBR alone. The very high number of hits under the TBR-ratchet approach, that is, always more than 96%, indicates that it is likely that the optimal trees were found (Ojanguren & Ramirez, 2009). Bootstrap and Bremer support (Felsenstein 1985; Bremer 1994) were also calculated, the former with default settings, the latter generated by increasing the tree buffer and the suboptimal threshold by steps in TNT. Starting with the four most parsimonious trees, a traditional search with 20 replicates was performed keeping 2000 trees with one step suboptimal (commands: mult 20; sub 1; hold 2000). Another 15 cycles followed, increasing the suboptimal bound by one and the tree buffer by 2000 in each run (commands: sub 2; hold 4000; sub 3; hold 6000;…; sub 16; hold 32000).

We used both equal and implied weighting, in the latter case applying a range of values for the concavity constant K (1, 2, 3 to 20, 25, 50 and 100). Which weighting strategy should be used in the parsimony framework remains an unresolved question (Kjer *et al.* 2007), as does the value to be chosen under implied weighting for the concavity constant K (Goloboff 1993; Turner & Zandee 1995). A common approach to circumvent this problem is to do a sensitivity analysis, showing how sensitive the support for different groups is to method and parameter choice (Wheeler 1995; Giribet 2003). We employ a different strategy, using congruence with the molecular topology as a guide to choose the best suited weighting strategy for the morphological data (Miyamoto & Fitch 1995; Cunningham 1997). To assess this congruence, we calculated the minimum SPR distances reached by any of the shortest trees using the program TNT (Goloboff *et al.* 2008). We compared all shortest trees found during parsimony analysis of the morphological data with the topology obtained from the partitioned Bayesian analysis of the combined molecular dataset. This approach identified implied weighting with $K = 9$ as the weighting strategy maximizing congruence with the independently derived molecular tree (Table 1).

Table 1 Topological distances between trees obtained under different analysis methods for morphology and between trees obtained from different data partitions

Morphological data	SPR min	SPR mean
Molecular tree – IW $K = 09$	32	33.22
Molecular tree – IW $K = 14$	33	33.90
Molecular tree – IW $K = 10$	33	33.95
Molecular tree – IW $K = 11$	33	33.95
Molecular tree – IW $K = 13$	33	33.96
Molecular tree – IW $K = 12$	33	34.00
Molecular tree – IW $K = 15$	33	34.00
Molecular tree – IW $K = 07$	33	34.14
Molecular tree – IW $K = 08$	34	35.05
Molecular tree – IW $K = 06$	35	35.20
Molecular tree – IW $K = 05$	35	35.28
Molecular tree – equal	35	38.22
Molecular tree – IW $K = 16$	36	36.55
Molecular tree – IW $K = 18$	36	36.67
Molecular tree – IW $K = 04$	36	37.03
Molecular tree – IW $K = 02$	36	37.33
Molecular data		
Total evidence – 28S		8
Total evidence – EF1a		15
Total evidence – mtDNA		9
28S – EF1a		15
28S – mtDNA		15
EF1a – mtDNA		18

SPR min, minimal SPR distance; SPR mean, average SPR distance; IW, implied weighting; Equal W, equal weighting; EF1a, elongation factor 1α.

Molecular and total evidence phylogenetic analyses

The molecular dataset was analysed using maximum-likelihood (ML) and Bayesian approaches. To assess the congruence between phylogenies obtained from independent datasets, we also analysed the mitochondrial genes (CO1 and ND1), 28S and EF1α separately.

We identified the best-fitting nucleotide substitution models using MrModeltest version 2.2 (Nylander 2004), with a neighbor-joining tree as the test tree and applying the Akaike information criterion (following Posada & Buckley 2004). The results of the model choice are shown in Table 2. We tested different partitioning strategies according to the method proposed by Brandley *et al.* (2005) and advocated by Brown & Lemmon (2007). Partitioning schemes are summarized in Appendix 3 and ranged from an unpartitioned analysis (P1) to a distinction of eight partitions chosen based on gene identity and prior knowledge of biochemical properties (P8): the pairing stem regions of 28S, its remaining loop regions, combined first and second codon positions of each of the three protein-coding genes (CO1, ND1 and EF1α) and finally their third codon position. To obtain an estimate for the Bayes factors associated with each comparison of partitioning strategies, we conducted a Bayesian MCMC analysis in MrBayes v.3.1.2 (Ronquist & Huelsenbeck 2003) for each partitioning strategy separately. Analyses were run with two independent runs of four chains each (heating $T = 0.1$), default prior settings, random starting trees and

Table 2 Data partitions, their properties and estimated models of sequence evolution

Partition	#bp	#var	pars	AT%	Model
CO1	648	320	269	73	GTR+I+Γ
CO1 first and second codon positions	432	123	84	63	GTR+I+Γ
CO1 third codon positions	216	197	185	93[a]	GTR+I+Γ
ND1	411	282	229	83	GTR+I+Γ
ND1 first and second codon positions	274	154	114	78	GTR+I+Γ
ND1 third codon positions	137	128	115	94	GTR+Γ
28S	568	216	128	39	GTR+I+Γ
28S stem	354	140	84	29	GTR+Γ (+doublet)
28S loop	214	76	44	56	SYM+I+Γ
EF1α	519	166	139	46	GTR+I+Γ
EF1α first and second codon positions	346	21	13	53	GTR+I+Γ
EF1α third codon positions	173	145	126	32	GTR+I+Γ
Morphology	–	–	66	–	Mk+Γ (var)
Combined dataset	2146	984	765	60	GTR+I+Γ

#bp, number of base pairs included in the analysis; #var, number of variable sites; #pars, number of parsimony informative sites; AT, AT content of the respective partition; Model, substitution model applied in the partitioned Bayesian analysis; EF1a, elongation factor 1α.

[a]Homogeneity test of base composition across taxa revealed a significant deviation from homogeneity ($P = 0.0024$).

trees sampled every 1000 generations for 5×10^6 generations. We then discarded half of the generations as a burn-in, and obtained estimates for the harmonic means of the likelihood scores from the remaining generations using the sump command implemented in MrBayes (Ronquist & Huelsenbeck 2003). The same procedure as for the partitioning strategies was applied to test whether the application of the doublet model as implemented in MrBayes (Schoeniger & von Haeseler 1994; Ronquist & Huelsenbeck 2003) significantly improved the phylogenetic estimation (P8*b; Appendix 3).

Final likelihood analyses were conducted using RaxML (Stamatakis *et al.* 2008) under a GTR+Γ+I model with 1000 random parsimony starting trees, applying the rapid hill-climbing algorithm, and adopting the partitioning strategy preferred by the Bayes factor comparison. Clade support was assessed by 1000 non-parametric bootstrap iterations, applying fast bootstrapping.

For the Bayesian estimates, separate and joint analyses were conducted running for 1×10^7 generations in the single-gene analyses and 4×10^7 generations in the combined molecular analysis. Convergence of the two parallel runs was checked in four ways. The log-likelihood scores (ln *L*) were plotted over generations and stabilization determined. The overlay plot of the two independent runs was examined for a good mixing of the runs and stabilization of the ln *L*. Then, we checked whether the standard deviation of split frequencies between the two runs fell below the 0.01 threshold (Ronquist & Huelsenbeck 2003). Finally, we studied the behaviour of the potential scale reduction factor (PSRF) for the model parameters and clade supports, and considered the runs to have converged if the PSRF was <5% divergent from 1. Convergence as assessed this way was always reached before one-third of the total number of generations, but we discarded half of the generations as a conservative burn-in.

The total evidence dataset, combining molecular and morphological characters, was analysed with parsimony under equal weights, under ML, and using a partitioned Bayesian approach, in each case with the settings and search strategies that are mentioned above for the separate analyses. For the morphological partition in both RaxML and MrBayes, we applied the MK model with equal state frequencies and transition rates, and a gamma distributed rate variation across characters. The coding bias was set to 'variable' in the MrBayes analysis.

Alternative hypotheses testing

Three out of 10 genera that were represented by more than one species were recovered as paraphyletic in all our analyses. To test whether this non-monophyly is statistically supported, we used both Bayesian and likelihood-based approaches. First, we evaluated whether there was at least one tree in the 95% confidence set of tree topologies, which showed any of the three genera in question to be monophyletic, which would mean that the Bayesian analysis could not exclude monophyly. To do so, we filtered the Bayesian topologies included in the 95% set of trees with a constraint topology that enforced the monophyly of the genera in question in PAUP* (Swofford 2002). Additionally, we applied the Shimodaira–Hasegawa test (Shimodaira & Hasegawa 1999) as implemented in PAUP*. Trees for testing were obtained by separately enforcing monophyly of all three genera in a Bayesian analysis, using the same settings as employed above. The SH tests were carried out

applying the resampling estimated log-likelihood method (Kishino *et al.* 1990) with 1000 replicates to create the test distribution.

Results

Phylogenetic reconstructions

The phylogenies as retrieved from analysing the morphological and the molecular data partition separately are shown in Fig. 3. While both independent datasets support the three genus groups found in a previous study (Klopfstein *et al.* 2010a), the relationships between these genus groups differ between the two analyses, as do some of the internal relationships. The largest differences are observed within the *Syrphoctonus* genus group, which shows a different sequence of genera (i.e. a different 'internal rooting' of the genus group) in the morphological vs. the molecular tree. The genera appearing as the most basal ones in the molecular tree, that is, *Syrphoctonus* s.str., *Enizemum* and *Woldstedtius*, are the most derived genera in the morphological tree, and the contrary applies to *Phthorima* and *Bioblapsis*. The support for these relationships is, however, very low in the morphological tree, with none of the conflicting nodes supported in the bootstrap analysis, and Bremer support values consistently lower than the ones found within the two other genus groups. The inter-generic relationships in the *Sussaba* and *Diplazon* genus groups are in less conflict between the two datasets. However, while the genus *Tymmophorus* is only supported by morphology (although not significantly rejected by molecules, see below), the genera *Promethes* and *Diplazon* are only supported by the molecular data.

To further assess congruence between trees resulting from morphology and from molecules, we compared the

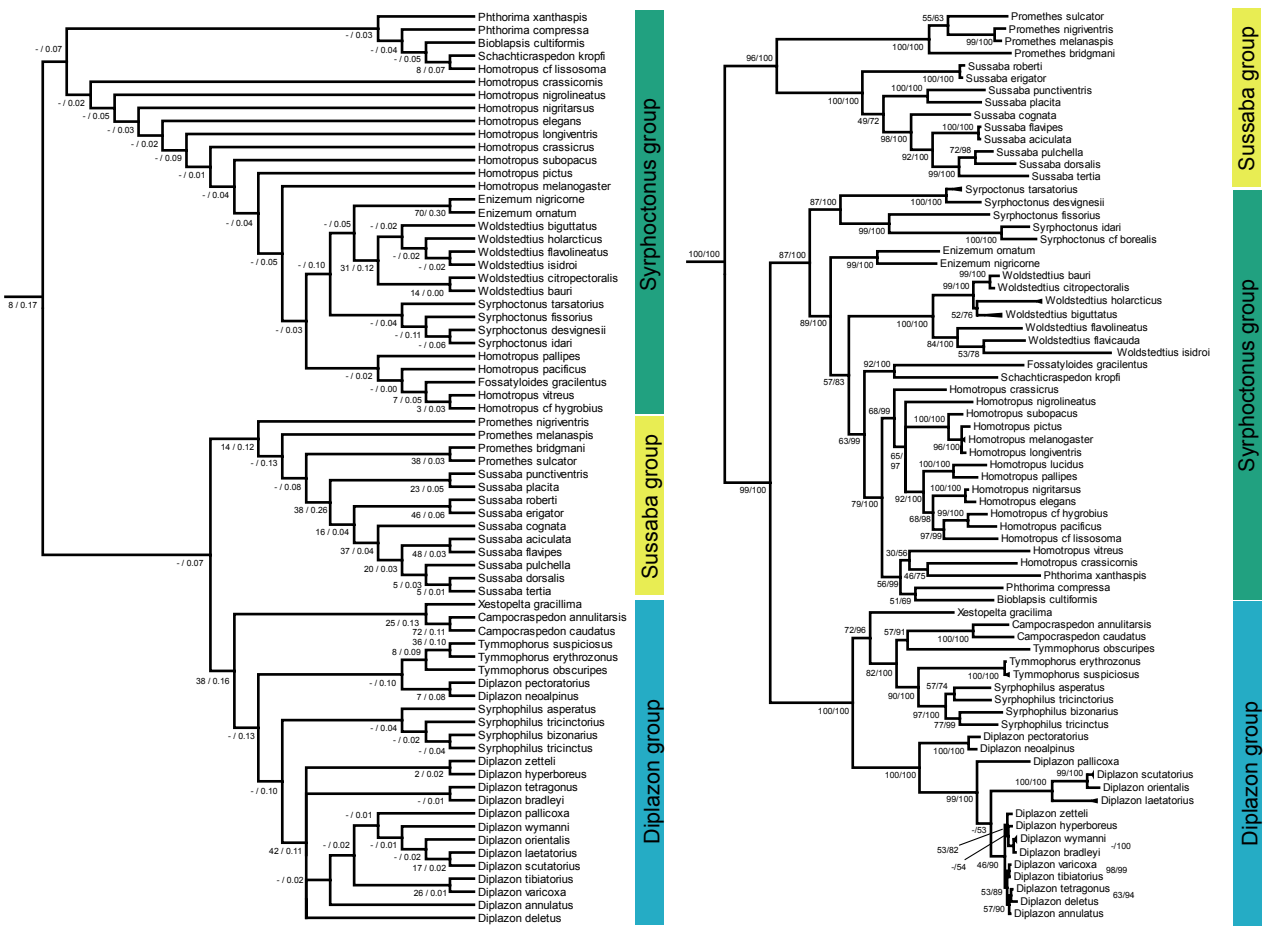

Fig. 3 Diplazontinae phylogeny as derived from morphology (A) and molecules (B) analysed separately. (A) Strict consensus of the four shortest trees resulting from the morphological partition alone, analysed under implied weighting ($K = 9$). Node labels represent maximum parsimony bootstrap support and Bremer support values. (B) Majority-rule consensus resulting from the Bayesian analysis of the molecular dataset alone. Node labels represent maximum likelihood bootstrap support and Bayesian posterior probabilities.

topological distance between the shortest tree obtained from morphology alone and the molecular tree to the distances between the topologies resulting from the three independent molecular data partitions. As shown in Table 1, congruence between the single genetic partitions (SPR distance between 28S and EF1a: 15, between 28S and mtDNA: 15, between EF1a and mtDNA: 18) was distinctly higher than between morphology and molecules (SPR distance 32 with implied weighting at $K = 9$ and 35 under equal weighting). To see which type of character contributed most to the morphological phylogeny, we calculated CI and RI for all the characters on the total evidence topology (Appendix 2). When splitting the morphological characters into structural, colour and sculpture characters, we found that the structural characters performed best (average CI = 0.34, average RI = 0.67), followed by colour (CI = 0.32, RI = 0.48) and sculpture characters (CI = 0.10, RI = 0.55) (the two behavioural characters had comparatively low average homoplasy levels, CI = 0.38, RI = 0.88). The differences were, however, not large and maximum indices were reached both by structural and colour characters, which also both provided synapomorphies for genus level and higher level groupings (see below). Only the sculpture characters had consistently higher levels of homoplasy.

One strategy to handle conflict between datasets is to analyse them in a combined analysis, and assess the relative contribution of the data partitions to the resulting tree (Wahlberg & Nylin 2003; Wahlberg *et al.* 2005; Brower 2009). The total evidence consensus tree resulting from the Bayesian analysis is shown in Fig. 4, along with bootstrap supports of the MP and ML analyses and Bayesian posterior probabilities. Additionally, for each node, we report the support of the four independent partitions, that is, the nuclear 28S and EF1α genes, the mitochondrial partition (CO1 and ND1), and the morphological dataset analysed using implied weighting with $K = 9$. The trees resulting from the analyses of the single partitions are provided as Supporting information. In cases where morphology and molecular analyses gave conflicting results (Fig. 3), the conflict was usually resolved in favour of the molecular dataset in the total evidence approach. This is especially the case for the relationships between the three genus groups and the placement of genera within the *Syrphoctonus* group.

However, morphology could become important in resolving the phylogeny in cases of conflict between the different molecular data partitions. Congruence between the different molecular data partitions was relatively high, and conflict between the topologies obtained by single-gene analyses generally involved weakly supported nodes. However, there are some noteworthy exceptions, for example, at the basis of the genus *Sussaba*. While 28S and mtDNA data place the species pair *Sussaba erigator* and *S. roberti* at the base of the genus, EF1a and morphology favour *Sussaba placita* plus *Sussaba punctiventris* as the most basal taxon in this genus. The addition of the morphological partition leads to a resolution of this conflict in favour of the latter possibility in the total evidence tree, which was not the case for the combined molecular analysis. Such a placement, however, also makes sense when including knowledge about the morphological variation found in related genera that were not included in this analysis (i.e. *Episemura* and *Eurytyloides*).

Overall, 66 of the possible 69 ingroup nodes are resolved on the Bayesian consensus tree of the total evidence analysis, and 52 nodes are supported by a posterior probability of at least 95%. Of these, 42 are also recovered by at least two independent partitions, of which 27 had posterior probabilities above 95%. Although generally highly resolved, the phylogeny also contains ambiguous relationships, for example, in the genus *Diplazon* Nees. Most of the species in this genus are of uncertain placement, support is generally low and only reached by combining all four data partitions. Because of a lack of variability, the nuclear data (28S and EF1α) contribute very little to resolution here, which might indicate a relatively young age of these species. To illustrate regions of low resolution or conflict on the phylogeny more accurately, we constructed a phylogenetic network based on the trees contained in the 95% set of Bayesian trees, estimated from the molecular data (Fig. 5). This network clearly shows that the basal splits of the phylogeny are tree-like, reflecting the high support values in that part of the phylogeny; regions with less stability involve the genus *Diplazon*, the relationships among genera and some species groups in the *Syrphoctonus* genus group, and the placement of *Xestopelta*.

Diplazontinae classification

The three genus groups obtained in the previous phylogenetic analysis of the subfamily (Klopfstein *et al.* 2010a) are confirmed with high support by the concatenated molecular analysis, and by most of the analyses of independent data partitions. The nuclear 28S and the mitochondrial partition support all three genus groups, while the phylogeny recovered by EF1α shows no resolution at the base of the *Sussaba* genus group and a nesting of the *Diplazon* genus group inside the *Syrphoctonus* group, but with low support (ML bootstrap support: 0.37; Bayesian posterior probability: 0.72). In the morphological analysis, all three genus groups were recovered, although with very low bootstrap supports. A number of synapomorphies of the three groups was revealed in the morphological analysis.

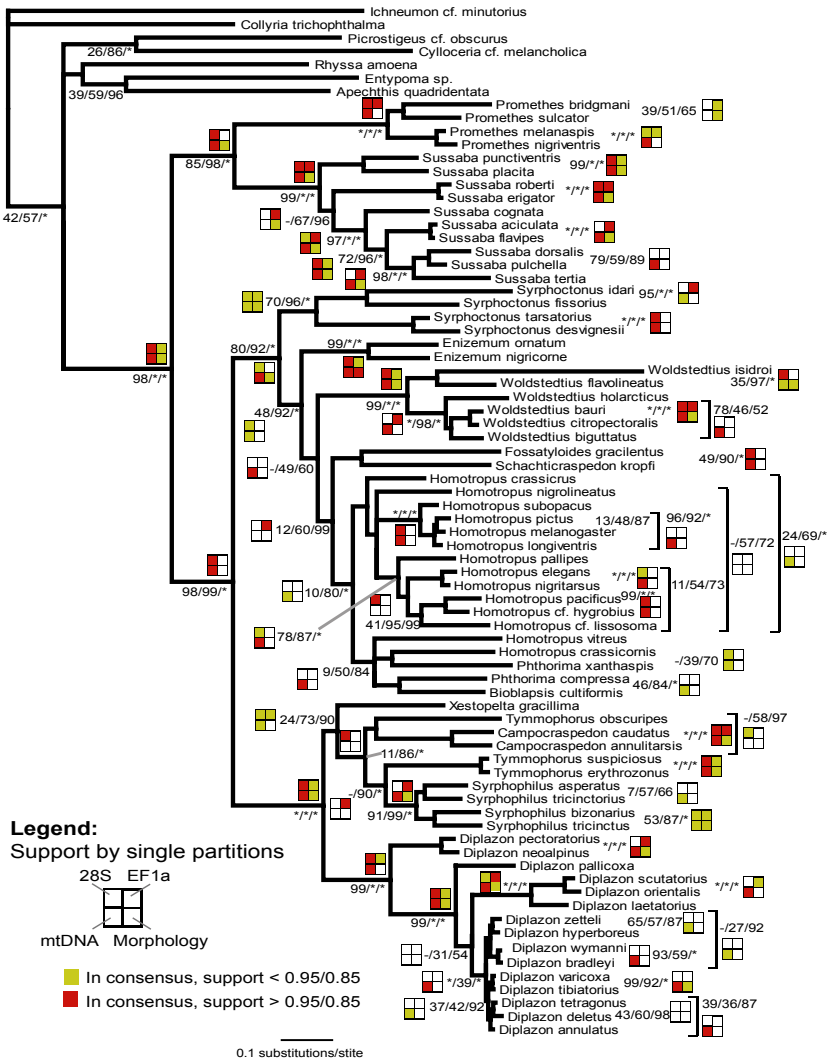

Fig. 4 Total evidence consensus tree resulting from the Bayesian analysis of four genes plus morphology. For each node, the support is given as parsimony bootstrap proportions, maximum likelihood bootstrap proportions and Bayesian posterior probabilities, respectively. A star represents maximum support (100%), a dash (–) means that the grouping was not present in the consensus tree. Additionally, the support by each of the four independent partitions is given as a colour code (see legend), i.e. by the nuclear 28S rRNA, by the nuclear EF1α, by the combined mitochondrial genes (CO1 and ND1) and by the morphological matrix. For the molecular partitions, we report the groups resulting from the Bayesian analyses, and detail whether the group was only present on the consensus tree, or if it actually reached significant support, i.e. a posterior probability above 95%. For the morphological partition, we show the results from the parsimony analysis under implied weighting with $K = 9$, and distinguish if the group was present on the consensus of the four shortest trees found, or if it also reached a bootstrap support of at least 85% (see legend).

The *Sussaba* genus group can be characterized by the carinate scutellum and the single-lobed ninth sternite of the males. In the *Syrphoctonus* genus group, males have the ninth and tenth tergite separate. In the *Diplazon* genus group, the ninth and tenth tergite of the male is fused to a syntergum, as it is in the *Sussaba* group, but the ninth sternite is bilobate as in the *Syrphoctonus* group; females usually have yellow inner eye margins. The placement of *Xestopelta* in the *Diplazon* genus group is unexpected, but highly supported by all single partitions. Morphological characters supporting this placement include the yellow inner eye margins of the female, the thickened clypeus which *Xestopelta* shares with *Campocraspedon* Uchida, and the fused ninth and tenth tergite in combination with a bilobate ninth sternite in the male. The tropical *Schachticraspedon* belongs to the *Syrphoctonus* genus group, where it clusters with the new genus *Fossatyloides*. This placement is not supported by morphology, which retrieves *Fossatyloides*

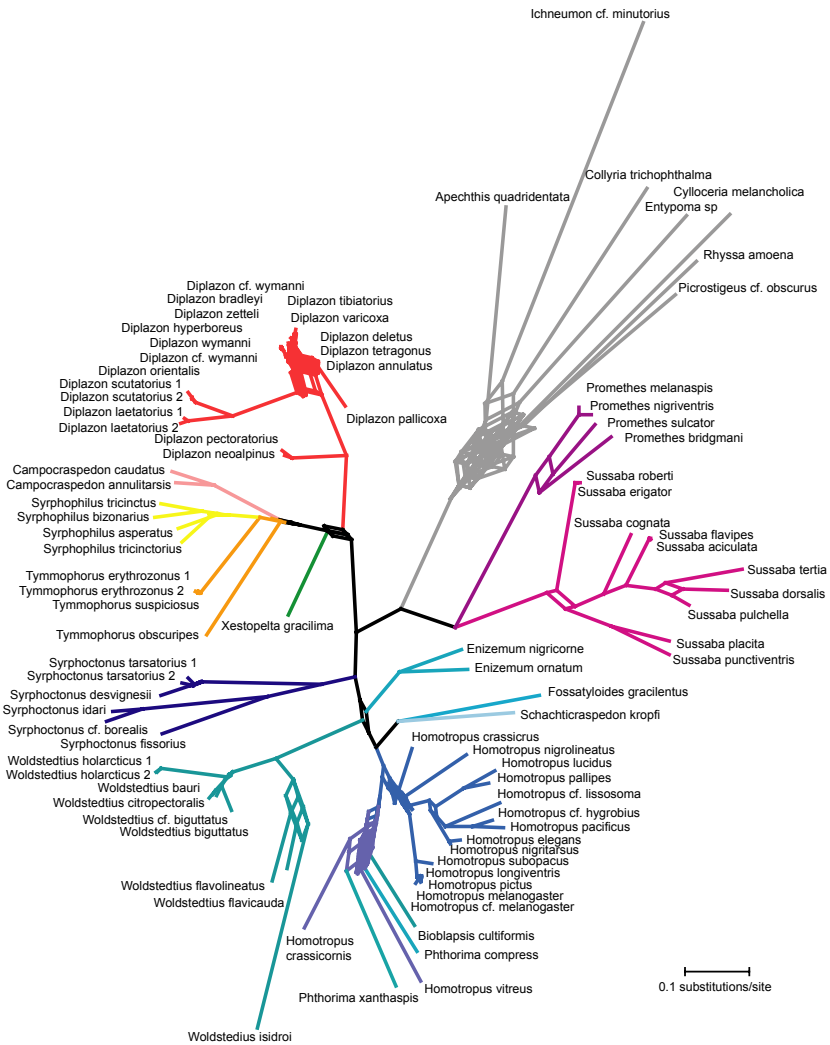

Fig. 5 Consensus network of 1000 trees sampled randomly from the Bayesian posterior distribution resulting from the combined molecular data. Branch colours represent the different genera.

as assuming a basal position within the genus group, but with low support. The remaining genera are placed as in the previous phylogenetic analysis of the subfamily (Klopfstein *et al.* 2010a).

Most of the genera included by multiple species in our analyses were recovered as monophyletic (Fig. 4), but three of them as paraphyletic (*Syrphoctonus*, *Tymmophorus*, *Phthorima* Förster). This was the case irrespective of whether morphology and molecules were analysed separately or in combination. The Bayesian approach to test their monophyly revealed no tree compatible with the constrained monophyly in the cases of *Syrphoctonus* and *Tymmophorus*, but 21 of 9111 trees from the 95% tree distribution had the genus *Phthorima* monophyletic (Table 3). The SH test (Shimodaira & Hasegawa 1999) only significantly rejected monophyly of *Syrphoctonus*. More information is therefore needed to clarify the status of these latter two genera. The paraphyly of *Syrphoctonus*, however, is highly corroborated, being supported by every single data partition. The genera *Bioblapsis* Förster, *Enizemum* Förster, *Phthorima*, *Schachticraspedon*, *Fossatyloides* gen. nov. and *Woldstedtius* Carlson are clearly nested within *Syrphoctonus* as currently defined, with the *tarsatorius* and *laevis* species groups as recognized by Dasch (1964) being basal to all other genera of the group and to the remaining *Syrphoctonus* species. As the type species of the genus is *Bassus exsultans* Gravenhorst (Yu & Horstmann 1997), a junior synonym of the here included *Syrphoctonus tarsatorius* (Panzer), we restrict the definition of *Syrphoctonus* to these groups of species. For the remaining species of *Syrphoct-*

Table 3 Results of the phylogenetic hypothesis testing

Taxon tested	SH test[a]	Bayesian filtering[b]
Phthorima	$P = 0.570$	21
Tymmophorus	$P = 0.572$	0
Syrphoctonus	$P < 0.001$*	0
Homotropus 1[c]	$P = 0.044$*	0
Homotropus 2[d]	$P = 0.299$	0
Homotropus 3[e]	$P = 0.860$	9054

[a]Shimodaira & Hasegawa (1999) test examining whether constraining for the monophyly of the tested taxon significantly decreases the likelihood of the resulting phylogeny.

[b]Bayesian filtering: number of trees found in the 95% range of trees from the Bayesian analysis that contain the tested taxon as monophyletic.

[c]Broadest definition of *Homotropus*, including all former *Syrphoctonus* species except for the *tarsatorius* and *fissorius* species groups.

[d]*Homotropus* defined as in c, but excluding *Fossatyloides gracilentus*.

[e]*Homotropus* defined as in d, but additionally excluding *Homotropus crassicornis* and *Homotropus vitreus*.

*Significantly rejected monophyly.

onus, the previously established genus *Homotropus* Förster is re-validated; its type species, *Homotropus elegans* (Gravenhorst), is shown by our analysis to be nested within the crown group of the remaining species. Dasch's species groups II–IV clearly form a monophyletic clade around *H. elegans*. However, from our phylogenetic analysis, it remains uncertain whether *Homotropus crassicornis* (Gravenhorst), *Homotropus vitreus* Dasch and *Fossatyloides gracilentus* (Holmgren) should also be included in *Homotropus*. To test whether they form part of this newly recognized genus, we performed additional alternative hypothesis testing, forcing three different definitions of *Homotropus* as monophyletic: (i) all species except the *tarsatorius* and *laevis* species groups or (ii) as before, but excluding *F. gracilentus*, and (iii) as before, but additionally excluding *H. crassicornis* and *H. vitreus*. According to these tests, *F. gracilentus* clearly does not form part of *Homotropus*, while the hypothesis that the other two doubtful species belong to this group cannot be rejected significantly based on our data (Table 3).

According to the results of the alternative hypotheses testing, we suggest the following changes to the generic definitions in the *Syrphoctonus* genus group: (i) the genus *Syrphoctonus* is restricted to the most basal clade consisting of the species *Syrphoctonus desvignesii* (Marshall), *S. fissorius* (Gravenhorst), *Syrphoctonus idari* Diller and *S. tarsatorius* (Panzer); (ii) the genus *Homotropus* with the type species *H. elegans* is revalidated (stat. rev.) to include *Homotropus crassicrus* Thomson (comb. n.), *H. elegans* (Gravenhorst) (comb. n.), *Homotropus longiventris* Thomson (comb. n.), *Homotropus melanogaster* (Holmgren) (comb. n.), *Homotropus nigritarsus* (Gravenhorst) (comb. n.), *Homotropus nigrolineatus* Strobl (comb. n.), *Homotropus pallipes* (Gravenhorst) (comb. n.), *Homotropus pictus* (Gravenhorst) (comb. n.), *Homotropus signatus* (Gravenhorst) (comb. n.), *Homotropus subopacus* (Stelfox) (comb. n.), and provisionally *H. crassicornis* (Gravenhorst) (comb. n.) and *H. vitreus* Dasch (comb. n.); (iii) a new genus, *Fossatyloides*, is described for *F. gracilentus* (comb. n.). Diagnoses and descriptions of the newly defined genera are provided in Appendix 4.

Discussion

Classification of Diplazontinae

Traditional generic concepts in Diplazontinae are largely confirmed by our phylogenetic analysis, a fact that is in agreement with a relatively good congruence between the phylogenies retrieved from the molecular and morphological data partitions. The only genus whose monophyly is in significant conflict with the total evidence phylogeny is *Syrphoctonus*. But this genus is not well defined morphologically either, which resulted in multiple appearances in the most recent generic key (Fitton & Rotheray 1982). The genus-level changes made here resolve some, but not all of these inconsistencies, and more data are needed to clarify the limits of the revalidated genus *Homotropus*. Additional taxon sampling should aim at including all the species groups proposed for the genus by Dasch (1964), as well as more species of *Phthorima* and *Bioblapsis*. Additional tropical genera which could not be included in our analyses, for example, *Syrphidepulo* Diller and *Extenuosodalis* Diller, might also cluster within this group, and should thus be included. No clear decision can currently be made about the status of *Tymmophorus* and *Phthorima*. However, they are both rather well defined by morphology, and should thus be retained until there is strong evidence against their monophyly.

The three genus groups previously recovered (Klopfstein *et al.* 2010a) are confirmed here. However, the present analysis cannot be regarded as independent from this previous analysis, as two of the genes were used in both studies. The EF1α data and the morphological partition, however, represent truly independent data and thus add to the corroboration of this hypothesis. Additional characters supporting the three genus groups stem from a recent analysis of courtship behaviour (Klopfstein *et al.* 2010b). Using a method to reproduce the antennal movement displayed by males during courtship in amputated antennae (Steiner *et al.* 2010), this analysis recorded data on antennal courtship in 64 diplazontine species. As a result, all examined males from the *Sussaba* group can be assumed to coil their antennae in a single coil around the antennae of the female. In the *Syrphoctonus* group, most males perform double-coiling, but two species are found to perform a form of single-coiling, and the genus *Woldstedtius* has lost

this behaviour. The *Diplazon* group finally seems to have lost this behaviour altogether. Single-coiling of the antennae could be a synapomorphy of the *Sussaba* group, although it might also represent the ancestral state in the subfamily, as it was shown by ancestral state reconstructions (Klopfstein *et al.* 2010b). Single-coiling is also found in two taxa of the *Syrphoctonus* group, *F. gracilentus* and in *H. vitreus*. However, it is probably not homologous to the single-coiling in the *Sussaba* group in these two taxa, as suggested by the different relative position of the coil when formed, which is upright in the case of the species of the *Sussaba* group, while it is turned downwards in the two unrelated species.

The high support for the three genus groups from independent datasets might suggest a formal description of them, for example, as tribes, to restore the phylogeny–classification link (Franz 2005; Assis 2009). However, the diplazontine genera that were not included in this study currently cannot be placed with certainty. We thus prefer to preliminarily address these taxa as informal genus groups and await further evidence especially from some of the rare and putatively basal genera (e.g. *Episemura* Kasparyan & Manukyan, *Eurytyloides* Nakanishi).

Morphology and molecules for diplazontine phylogenetics

The here-proposed phylogenetic hypothesis of Diplazontinae is in large agreement with the only previous phylogenetic study of the group (Klopfstein *et al.* 2010a). The additional taxon and data sampling increased the support for some of the major groups found in the previous study, brought a better understanding of the inter-generic relationships in the *Diplazon* genus group, and resolved the hitherto ambiguous basal relationships inside the genus *Sussaba*. The inclusion of *Schachticraspedon* helped in resolving the phylogenetic position of *F. gracilentus*, which, in the previous analysis, clustered basal to the genus *Enizemum*, but with low support.

Due to its high resolution and support by independent data partitions, this phylogeny constitutes a robust framework for both classification and comparative studies. In ichneumonids, and also in other groups of parasitoid wasps, phylogenies with dense taxon coverage at the species level are still scarce; but, such phylogenies are needed to understand the evolution of life history characteristics and host associations. The Diplazontinae might be especially yielding in this respect, as they exhibit a tight association with their hosts. It has been shown that the timing of pupation of the Syrphinae hosts is solely regulated by the parasitoid (Schneider 1948); the physiological interactions between host and parasitoid thus appear to be intense. Furthermore, the degree of specialization varies a lot between species, with some only being reared from single host species, while others can develop in syrphine species that are only distantly related (Rotheray 1984).

The role of morphological characters in phylogenetics is extensively discussed, especially now that molecular data are accumulating at an unprecedented speed (e.g. Baker *et al.* 1998; Scotland *et al.* 2003; Wiens 2004; Wortley & Scotland 2006; Assis 2009). In our phylogenetic analysis, the morphological partition only played a minor role in resolving the phylogeny, as shown by the fact that the topology only changed little when the morphological partition was added to the molecular data in a total evidence approach. Most of the conflicts between morphology and molecules were resolved according to the molecular partition in the total evidence tree, and morphology only had an influence in a few cases where molecular data alone only delivered low support for relationships, for example, because of conflict between the single-gene trees.

The relatively low contribution of morphology could either reflect a general pattern as it was found in a review of 26 total evidence analyses (Wortley & Scotland 2006), or it could indicate that our morphological dataset was not sufficient to overcome the molecular evidence. Actually, the number of characters included is rather low considering the number of taxa; moreover, there seems to be a lack of good characters to structure the relationships within the *Syrphoctonus* group, as indicated by the relatively low clade support values achieved there. On the other hand, parasitoid wasps are known for relatively high levels of morphological homoplasy, which, at least in part, seems to be caused by convergent adaptations to a specific host niche (Gauld & Mound 1982; Quicke & Belshaw 1999; Laurenne *et al.* 2009). Such an effect was evident in our dataset in the case of the shape of the female metasoma, which is laterally or dorso-ventrally compressed in several not closely related species or groups. Moreover, the subfamily Diplazontinae is morphologically rather uniform, and structural characters that can be coded unambiguously are rather scarce. The dense sampling at the species level poses the additional problem of finding characters with enough variation between closely related, but not within species.

Whether additional characters, for example, from ultrastructural investigations or using internal morphology, would change this situation is difficult to predict. In any case, only judging the contribution of morphology based on reached support values disregards the fact that morphological data have other distinct advantages over molecules. One of the most prominently mentioned advantages is the larger number of taxa accessible to morphological studies. When reconstructing the phylogeny of species-rich taxa such as insects, researchers usually obtain fresh material to extract DNA only for a small fraction of the known diver-

sity. Many species are only known from few individuals, in the extreme only from the holotype. Phylogenies that only cover part of the taxonomic diversity are, however, of limited use for taxonomic revisions and for the testing of evolutionary hypotheses (Zhang & Nei 1997; Pollock & Bruno 2000; Heath *et al.* 2008b). Moreover, the positive effects of an increased taxon sampling on phylogenetic accuracy are widely acknowledged (Graybeal 1998; Sullivan *et al.* 1999; Hillis *et al.* 2003; Hedtke *et al.* 2006; Heath *et al.* 2008a; Goloboff *et al.* 2009). Another important advantage of the continued use of morphology in phylogenetic is that it can bridge the gap to classification. Defining species or higher level taxa based on a molecular phylogenies alone is problematic on both philosophical and practical grounds (Jenner 2004; Wiens 2004; Schlick-Steiner *et al.* 2007). Moreover, morphological synapomorphies are needed to allow placement of taxa for which no molecular data are available.

Acknowledgements

We thank Nina Laurenne and the Swedish Malaise Trap Project for providing a large part of the specimens. Some additional specimens and data were provided by National Science Foundation grant BSI-07-17458 to Scott R. Shaw (Wyoming). We thank J. Salvador Arias, Pablo Goloboff and an anonymous reviewer for useful comments on a previous version of this manuscript. This research received support from the SYNTHESYS Project http://www.synthesys.info which is financed by European Community Research Infrastructure Action under the FP6 'Structuring the European Research Area' Programme. This study was partly supported by a grant from the Roche Research Foundation to SK and by NE/C519583 grant from the Natural Environment Research Council to DLQ (and to Prof. Andy Purvis).

References

Assis, L. C. S. (2009). Coherence, correspondence, and the renaissance of morphology in phylogenetic systematics. *Cladistics*, *25*, 528–544.

Baker, R. H., Yu, X. & DeSalle, R. (1998). Assessing the relative contribution of molecular and morphological characters in simultaneous analysis trees. *Molecular Phylogenetics and Evolution*, *9*, 427–436.

Beirne, B. P. (1941). British species of Diplazonini (Bassini auctt.) with a study of the genital and postgenital abdominal sclerites in the male. *Transactions of the Royal Entomological Society, London*, *91*, 661–712.

Belshaw, R. & Quicke, D. L. J. (1997). A molecular phylogeny of the Aphidiinae (Hymenoptera: Braconidae). *Molecular Phylogenetics and Evolution*, 7, 281–293.

Brandley, M. C., Schmitz, A. & Reeder, T. W. (2005). Partitioned Bayesian analyses, partition choice, and the phylogenetic relationships of scincid lizards. *Systematic Biology*, *54*, 373–390.

Bremer, K. (1994). Branch support and tree stability. *Cladistics*, *10*, 295–304.

Brower, A. V. Z. (2009). Combining data in phylogenetic analysis. *Trends in Ecology & Evolution*, *11*, 334–335.

Brown, J. M. & Lemmon, A. R. (2007). The importance of data partitioning and the utility of Bayes factors in Bayesian phylogenetics. *Systematic Biology*, *56*, 643–655.

Carpenter, J. M. & Wheeler, W. C. (1999). Towards simultaneous analysis of morphological and molecular data in Hymenoptera. *Zoologica Scripta*, *28*, 251–260.

Cunningham, C. W. (1997). Is congruence between data partitions a reliable predictor of phylogenetic accuracy? Empirically testing an iterative procedure for choosing among phylogenetic methods. *Systematic Biology*, *46*, 464–478.

Danforth, B. N. & Ji, S. (1998). Elongation factor-1α occurs as two copies in bees: implications for phylogenetic analysis of EF-1α sequences in insects. *Molecular Biology and Evolution*, *15*, 225–235.

Dasch, C. E. (1964). Ichneumon-flies of America north of Mexico 5: subfamily Diplazontinae. *Memoirs of the American Entomological Institute*, *3*, 1–304.

Dusek, J., Láska, P. & Sedivy, J. (1979). Parasitization of aphidophagous Syrphidae (Diptera) by Ichneumonidae (Hymenoptera) in the Palaearctic Region. *Acta Entomologica Bohemoslovaca*, *76*, 366–378.

Felsenstein, J. (1985). Confidence limits on phylogenies: an approach using the bootstrap. *Evolution*, *39*, 783–791.

Fitton, M. G. & Rotheray, G. E. (1982). A key to the European genera of diplazontine ichneumon-flies, with notes on the British fauna. *Systematic Entomology*, 7, 311–320.

Folmer, O., Black, M., Hoeh, W., Lutz, R. & Vrijenhoek, R. (1994). DNA primers for amplification of mitochondrial cytochrome c oxidase subunit I from diverse metazoan invertebrates. *Molecular Marine Biology and Biotechnology*, *3*, 294–299.

Franz, N. M. (2005). On the lack of good scientific reasons for the growing phylogeny/classification gap. *Cladistics*, *21*, 495–500.

Gauld, I. D. & Mound, L. A. (1982). Homoplasy and the delineation of holophyletic genera in some insect groups. *Systematic Entomology*, 7, 73–86.

Gillespie, J. J., Yoder, M. J. & Wharton, R. A. (2005). Predicted secondary structure for 28S and 18S rRNA from Ichneumonoidea (Insecta: Hymenoptera: Apocrita): impact on sequence alignment and phylogeny estimation. *Journal of Molecular Evolution*, *61*, 114–137.

Giribet, G. (2003). Stability in phylogenetic formulations and its relationship to nodal support. *Systematic Biology*, *52*, 554–564.

Goloboff, P. A. (1993). Estimating character weightings during tree search. *Cladistics*, *9*, 83–91.

Goloboff, P. A., Farris, J. S. & Nixon, K. C. (2008). TNT, a free program for phylogenetic analysis. *Cladistics*, *24*, 774–786.

Goloboff, P. A., Catalano, S. A., Mirande, J. M., Szumik, C. A., Arias, J. S., Källersjö, M. & Farris, J. S. (2009). Phylogenetic analysis of 73 060 taxa corroborates major eukaryotic groups. *Cladistics*, *25*, 211–230.

Graybeal, A. (1998). Is it better to add taxa or characters to a difficult phylogenetic problem? *Systematic Biology*, *47*, 9–17.

Heath, T. A., Hedtke, S. M. & Hillis, D. M. (2008a). Taxon sampling and the accuracy of phylogenetic analyses. *Journal of Systematics and Evolution*, *46*, 239–257.

Heath, T. A., Zwickl, D. J., Kim, J. & Hillis, D. M. (2008b). Taxon sampling affects inferences of macroevolutionary processes from phylogenetic trees. *Systematic Biology*, *57*, 160–166.

Hedtke, S. M., Townsend, T. M. & Hillis, D. M. (2006). Resolution of phylogenetic conflict in large data sets by increased taxon sampling. *Systematic Biology*, *55*, 522–529.

Hillis, D. M., Pollock, D. D., McGuire, J. A. & Zwickl, D. J. (2003). Is sparse taxon sampling a problem for phylogenetic inference? *Systematic Biology*, *52*, 124–126.

International Commission on Zoological Nomenclature (1999). *International Code of Zoological Nomenclature*. London: The International Trust for Zoological Nomenclature.

Jenner, R. A. (2004). Accepting partnership by submission? Morphological phylogenetics in a molecular millennium. *Systematic Biology*, *53*, 333–342.

Jones, O. R., Purvis, A., Baumagart, E. & Quicke, D. L. J. (2009). Using taxonomic revision data to estimate the geographic and taxonomic distribution of undescribed species richness in the Braconidae (Hymenoptera: Ichneumonoidea). *Insect Conservation and Diversity*, *2*, 204–212.

Kamal, M. (1926). A study of some hymenopterous parasites of aphidophagous Syrphidae. *Journal of Economic Entomology*, *19*, 721–730.

Katoh, K., Asimenos, G. & Toh, H. (2009). Multiple alignment of DNA sequences with MAFFT. *Methods in Molecular Biology*, *537*, 39–64.

Kishino, H., Miyata, T. & Hasegawa, M. (1990). Maximum likelihood inference of protein phylogeny and the origin of chloroplasts. *Journal of Molecular Evolution*, *30*, 151–160.

Kjer, K. M., Swigonova, Z., LaPolla, J. S. & Broughton, R. E. (2007). Why weight? *Molecular Phylogenetics and Evolution*, *43*, 999–1004.

Klopfstein, S., Kropf, C. & Quicke, D. L. J. (2010a). An evaluation of phylogenetic informativeness profiles and the molecular phylogeny of Diplazontinae (Hymenoptera, Ichneumonidae). *Systematic Biology*, *59*, 226–241.

Klopfstein, S., Quicke, D. L. J. & Kropf, C. (2010b). The evolution of antennal courtship in diplazontine parasitoid wasps (Hymenoptera, Ichneumonidae, Diplazontinae). *BMC Evolutionary Biology*, *10*, 218.

Laurenne, N. M., Karatolos, N. & Quicke, D. L. J. (2009). Hammering homoplasy: multiple gains and losses of vibrational sounding in cryptine wasps (Insecta: Hymenoptera: Ichneumonidae). *Biological Journal of the Linnean Society*, *96*, 82–102.

Mardulyn, P. & Whitfield, J. B. (1999). Phylogenetic signal in the COI, 16S, and 28S genes for inferring relationships among genera of Microgastrinae (Hymenoptera; Braconidae): evidence of a high diversification rate in this group of parasitoids. *Molecular Phylogenetics and Evolution*, *12*, 282–294.

Miyamoto, M. M. & Fitch, W. M. (1995). Testing species phylogenies and phylogenetic methods with congruence. *Systematic Biology*, *44*, 64–76.

Ngamo Tinkeu, L. S. & Hance, T. (1997). Reduction of predatory efficiency of hoverflies (Diptera, Syrphidae) in cereal fields due to parasitism. *Mededelingen Faculteit Landbouwkundige En Toegepaste Biologische Wetenschappen Universiteit Gent*, *62*, 469–472.

Nylander, J. A. A. 2004. *MrModeltest v2: Program distributed by the author*. Evolutionary Biology Centre, Uppsala University, Uppsala.

Ojanguren-Affilastro, A. A. & Ramirez, M. J. (2009). Phylogenetic analysis of the scorpion genus Brachistostemus (Arachnida, Scorpiones). *Zoologica Scripta*, *38*, 183–198.

Page, R. D. M. & Charleston, M. A. (1998). Trees within trees: phylogeny and historical associations. *Trends in Ecology & Evolution*, *13*, 356–359.

Patterson, C., Williams, D. M. & Humphries, C. J. (1993). Congruence between molecular and morphological phylogenies. *Annual Review of Ecology and Systematics*, *24*, 153–188.

Pollock, D. D. & Bruno, W. J. (2000). Assessing an unknown evolutionary process: effect of increasing site-specific knowledge through taxon addition. *Molecular Biology and Evolution*, *17*, 1854–1858.

Posada, D. & Buckley, T. R. (2004). Model selection and model averaging in phylogenetics: advantages of Akaike information criterion and Bayesian approaches over likelihood ratio tests. *Systematic Biology*, *53*, 793–808.

Quicke, D. L. J. (1997). *Parasitic Wasps*. London: Chapman and Hall.

Quicke, D. L. J. & Belshaw, R. (1999). Incongruence between morphological data sets: an example from the evolution of endoparasitism among parasitic wasps (Hymenoptera: Braconidae). *Systematic Biology*, *48*, 436–454.

Quicke, D. L. J., Laurenne, N. M., Fitton, M. G. & Broad, G. R. (2009). A thousand and one wasps: a 28S rDNA and morphological phylogeny of the Ichneumonidae (Insecta: Hymenoptera) with an investigation into alignment parameter space and elision. *Journal of Natural History*, *43*, 1305–1421.

Ronquist, F. & Huelsenbeck, J. P. (2003). MrBayes 3: Bayesian phylogenetic inference under mixed models. *Bioinformatics*, *19*, 1572–1574.

Rotheray, G. E. (1981). Host searching and oviposition behaviour of some parasitoids of aphidophagous Syrphidae. *Ecological Entomology*, *6*, 79–87.

Rotheray, G. E. (1984). Host relations, life cycles and multiparasitism in some parasitoids of aphidophagous Syrphidae (Diptera). *Ecological Entomology*, *9*, 303–310.

Rotheray, G. E. (1990). A new species of *Bioblapsis* (Hymenoptera: Ichneumonidae) from Scotland parasitising a mycophagous hoverfly, *Cheilosia longula* (Diptera: Syrphidae). *Entomologica Scandinavica*, *21*, 277–280.

Schlick-Steiner, B. C., Seifert, B., Stauffer, C., Christian, E., Crozier, R. H. & Steiner, F. M. (2007). Without morphology, cryptic species stay in taxonomic crypsis following discovery. *Trends in Ecology & Evolution*, *22*, 391–392.

Schneider, F. (1948). Beirag zur Kenntnis der Generationsverhältnisse und Diapause räuberischer Schwebfliegen (Syrphidae, Dipt.). *Mitteilungen der Schweizerischen Entomologischen Gesellschaft*, *21*, 249–285.

Schoeniger, M. & von Haeseler, A. (1994). A stochastic model and the evolution of autocorrelated DNA sequences. *Molecular Phylogenetics and Evolution*, *3*, 240–247.

Scotland, R. W., Olmstead, R. G. & Bennett, J. R. (2003). Phylogeny reconstruction: the role of morphology. *Systematic Biology*, *52*, 539–548.

Shimodaira, H. & Hasegawa, M. (1999). Multiple comparisons of log-likelihoods with applications to phylogenetic inference. *Molecular Biology and Evolution*, *16*, 1114–1116.

Smith, P. T., Kambhampati, S., Völkl, W. & Mackauer, M. (1999). A phylogeny of aphid parasitoids (Hymenoptera: Braconidae: Aphidiinae) inferred from mitochondrial NADH1 dehydrogenase gene sequence. *Molecular Phylogenetics and Evolution*, *11*, 236–245.

Stamatakis, A., Hoover, P. & Rougemont, J. (2008). A rapid bootstrap algorithm for the RAxML web servers. *Systematic Biology*, *57*, 758–771.

Steiner, S., Kropf, C., Graber, W., Nentwig, W. & Klopfstein, S. (2010). Antennal courtship and functional morphology of tyloids in the parasitoid wasp *Syrphoctonus tarsatorius* (Hymenoptera: Ichneumonidae: Diplazontinae). *Arthropod Structure & Development*, *39*, 33–40.

Sullivan, J., Swofford, D. L. & Naylor, G. J. P. (1999). The effect of taxon sampling on estimating rate heterogeneity parameters of maximum-likelihood models. *Molecular Biology and Evolution*, *16*, 1347–1356.

Swofford, D. L. (2002). *PAUP*. Phylogenetic Analysis Using Parsimony (*and Other Methods): Version 4*. Sunderland, MA: Sinauer Associates.

Townes, H. K. (1969). The genera of Ichneumonidae, Part 1. *Memoirs of the American Entomological Institute*, *11*, 1–300.

Townes, H. K. (1971). The genera of Ichneumonidae, Part 4. *Memoirs of the American Entomological Institute*, *17*, 1–372.

Turner, H. & Zandee, R. (1995). The behaviour of Goloboff's tree fitness measure F. *Cladistics*, *11*, 57–72.

Wahl, D. B. (1990). A review of the mature larvae of Diplazontinae, with notes on larvae of Acaenitinae and Orthocentrinae and proposal of two new subfamilies (Insecta: Hymenoptera, Ichneumonidae). *Journal of Natural History*, *24*, 27–52.

Wahl, D. B. & Gauld, I. D. (1998). The cladistics and higher classification of the Pimpliformes (Hymenoptera: Ichneumonidae). *Systematic Entomology*, *23*, 265–298.

Wahlberg, N. & Nylin, S. (2003). Morphology versus molecules: resolution of the positions of Nymphalis, Polygonia, and related genera (Lepidoptera: Nymphalidae). *Cladistics*, *19*, 213–223.

Wahlberg, N., Braby, M. F., Brower, A. V. Z., de Jong, R., Lee, M.-M., Nylin, S. *et al.* (2005). Synergistic effects of combining morphological and molecular data in resolving the phylogeny of butterflies and skippers. *Proceedings of the Royal Society of London Series B-Biological Sciences*, *272*, 1577–1586.

Wheeler, W. C. (1995). Sequence alignment, parameter sensitivity, and the phylogenetic analysis of molecular data. *Systematic Biology*, *44*, 321–331.

Wiens, J. J. (2004). The role of morphological data in phylogeny reconstruction. *Systematic Biology*, *53*, 653–661.

Wortley, A. H. & Scotland, R. W. (2006). The effect of combining molecular and morphological data in published phylogenetic analyses. *Systematic Biology*, *55*, 677–685.

Yu, D. S. & Horstmann, K. (1997). A catalogue of world Ichneumonidae (Hymenoptera). *Memoirs of the American Entomological Institute*, *58*, 1558.

Yu, D. S., van Achterberg, K. & Horstmann, K. 2005. *World Ichneumonoidea 2004 – Taxonomy, Biology, Morphology and Distribution*. Canada: Vancouver. Available via http://www.taxapad.com.

Zhang, J. & Nei, M. (1997). Accuracies of ancestral amino acid sequences inferred by the parsimony, likelihood, and distance methods. *Journal of Molecular Evolution*, *44*, S139–S146.

Appendix 1 List of specimens including collection data and GenBank accession numbers

Taxon	Int. code	Collection[a]	Country/Department/Locality/Coordinates/Collection date	GenBank accession numbers			
				28S D2-3	EF1α	CO1	ND1
Diplazontinae							
Bioblapsis cultiformis	SK_2-D12	NMBE	Switzerland/Graubünden/Sur, NE Sur/46°52.419′N, 9°63.425′E/27.VII.-14.VIII.2006	FJ556489	GU597598	FJ556422	GU597688
Campocraspedon annulitarsis	SK_5_1	SMTP	Sweden/Up/Häbo kommun, Biskops-Arnö, northern beach/59°40.328′N, 17°30.051′E/19.VIII.-07.IX.2003	GU597538	GU597599	GU597778	GU597689
Campocraspedon caudatus	SK_1-C2	NMBE	Switzerland/Graubünden/Sur, Claveina/46°52.037′N, 9°65.645′E/16.-23.VI.2003	GU597539	GU597600	GU597779	GU597690
Diplazon annulatus	SK_1-A2	NMBE	Switzerland/Graubünden/Sur, NE Sur/46°52.419′N, 9°63.425′E/15.-20.VII.2006	FJ556492	GU597601	FJ556425	GU597691
Diplazon bradleyi	SK_2-A5	NMBE	USA/Alaska/Fairbanks, North Star Borough/20.-24.VI.2006	FJ556493	GU597602	FJ556426	GU597692
Diplazon deletus	SK_1-A8	NMBE	Switzerland/Graubünden/Sur, Dafora/46°52.470′N, 9°64.591′E/23.-30.VI.2003	FJ556495	GU597603	FJ556428	GU597693
Diplazon hyperboreus	SK_6_19	SMTP	Sweden/Up/Älvkarleby kommun, Bätfors/60°27.639′N, 17°19.069′E/27.VI.-01.VII.2004	GU597540	GU597604	GU597780	GU597694

Appendix 1 (Continued)

Taxon	Int. code	Collection[a]	Country/Department/Locality/ Coordinates/Collection date	GenBank accession numbers			
				28S D2-3	EF1α	CO1	ND1
Diplazon laetatorius	SK_1-C4	NMBE	Switzerland/Graubünden/Sur, NE Sur/46°52.419′N, 9°63.425′E/1.-25.IX.2006	FJ556496	GU597605	FJ556429	GU597695
D. laetatorius	SK_1-C5	NMBE	USA/Maryland/VII.2006	FJ556497	GU597606	FJ556430	GU597696
Diplazon neoalpinus	SK_5_2	NMBE	Switzerland/Glarus/Linthal, Obersand, Melchplatz/46°83.979′N, 8°9.3035E/19.-28.VI.2008	GU597541	GU597608	GU597781	GU597698
Diplazon orientalis	SK_7_1	NMBE	Thailand/Buri Prov./Kanchara, Thongpapoom, Chemical Farm/13.VI.2009	GU597542	GU597610	GU597782	GU597700
Diplazon pallicoxa	SK_5_3	NMBE	Switzerland/Bern/Bremgartenwald, Nägelisbode/ 46°96.592′N, 7°41.761E/27.VI.-8.VII.2008	GU597543	GU597611	GU597783	GU597701
Diplazon pectoratorius	SK_1-C6	NMBE	Switzerland/Graubünden/Sur, Dafora/46°52.470′N, 9°64.591′E/14.-21.VII.2003	GU597544	GU597612	FJ556433	GU597702
Diplazon scutatorius	SK_1-A11	NMBE	Finland/Southern Finland/Sipoonkorpi/16.-21.VI.2006	FJ556502	GU597613	FJ556435	GU597703
D. scutatorius	SK_2-E3	NMBE	Switzerland/Bern/Bremgartenwald/ 46°95.962′N, 7°41.565E/15.IX.-4.X.2006	FJ556503	GU597614	FJ556436	GU597704
Diplazon tetragonus	SK_1-B1	NMBE	Finland/Southern Finland/Sipoonkorpi/2.-12.VII.2006	FJ556504		FJ556437	GU597706
D. tetragonus	SK_2-A10	NMBE	Finland/Southern Finland/Sipoon, Hindsby/10.-18.VI.2005		GU597616		
Diplazon tibiatorius	SK_1-B2	NMBE	Switzerland/Graubünden/Sur, NE Sur/46°52.419′N, 9°63.425′E/19.-27.VII.2006	FJ556507	GU597617	FJ556440	GU597707
Diplazon varicoxa	SK_1-B4	NMBE	Switzerland/Graubünden/Sur, NE Sur/46°52.419′N, 9°63.425′E/1.-25.IX.2006	FJ556509	GU597618	FJ556442	GU597708
Diplazon wymanni	SK_6_17	SMTP	Sweden/BD/Gällivare kommun, Ätnarova försökspark, Pelttovaara/67°03.103′N, 20°23.154′E/29.VII.-13.VIII.2004	GU597547	GU597609	GU597784	GU597699
D. cf. *wymanni*	SK_3-D1	NMBE	Switzerland/Graubünden/Sur, Lai Neir/46°53.56′N, 9°63.739′E/7.-15.VII.2006	GU597545	GU597619	GU597786	GU597709
D. cf. *wymanni*	SK_6_16	SMTP	Sweden/Sk/Klippans kommun, Skäralid, valley below northern Liema/56°01.633′N, 13°13.406′E/14.VII.-06.VIII.2004	GU597546	GU597607	GU597785	GU597697
Diplazon zetteli	SK_1-A3	NMBE	Switzerland/Graubünden/Sur, Claveina/46°52.037′N, 9°65.645′E/2.-9.VI.2003	GU597548	GU597615	GU597787	GU597705
Enizemum nigricorne	SK_5_5	SMTP	Sweden/VB/Vindelns kommun, Kulbäckslidens försökspark, Gammnybränna/64°08.688′N, 19°35.335′E/01.-18.VIII.2003	GU597553	GU597624	GU597792	GU597714
Enizemum ornatum	SK_1-B5	NMBE	Switzerland/Graubünden/Sur, Claveina/46°52.037′N, 9°65.645′E/30.VI.-7.VII.2003	FJ556511	GU597625	FJ556444	GU597715
Fossatyloides gracilentus	SK_1-E12	NMBE	Switzerland/Graubünden/Sur, Dafora/46°52.470′N, 9°64.591′E/21.-28.VII.2003	FJ556526	GU597647	FJ556459	GU597737
Homotropus crassicornis	SK_5_10	SMTP	Sweden/Sö/Huddinge kommun, Sofielunds atervinningsanläggning/59°10.592N, 17°59.631E/30.VI.-13.VII.2004	GU597565	GU597642	GU597805	GU597732
Homotropus crassicrus	SK_4-C8	SMTP	Sweden/Sm/Nybro kommun, Alsterbro/Alsteran/63°12.220′N, 15°06.997′E/4.VII.-10.VII.2006	GU597566	GU597643	GU597806	GU597733
Homotropus elegans	SK_5_11	SMTP	Sweden/Vb/Vindelns kommun, Kulbäcken meadow/64°11.413′N, 19°36.342′E/01.-18.VIII.2003	GU597567	GU597645	GU597807	GU597735

Appendix 1 (Continued)

Taxon	Int. code	Collection[a]	Country/Department/Locality/ Coordinates/Collection date	GenBank accession numbers			
				28S D2-3	EF1α	CO1	ND1
Homotropus cf. *hygrobius*	SK_5_13	SMTP	Sweden/Sö/Trosa kommun, Hunga Södergard/58°55.244′N, 17°31.274′E/11.IX.-02.X.2004	GU597573	GU597657	GU597815	GU597747
Homotropus longiventris	SK_1-G5	NMBE	Switzerland/Solothurn/Trimbach, Miesernbach/47°36.498′N, 7°86.931′E/6.-13.VI.2002	GU597568	GU597649	GU597810	GU597739
Homotropus melanogaster	SK_4-E6	SMTP	Sweden/BD/Gallivare kommun, Atnarova försökspark, Pelttovaara/67°03.103′N, 20°23.154′E/8.VII.-29.VII.2004	GU597569		GU597811	
H. melanogaster	SK_6_39	SMTP	Sweden/Ög/Ödeshögs kommun, Omberg, Bokskogsreservatet/58°17.831′N, 14°38.089′E/5.-19.VII.2005		GU597650		GU597740
H. cf. *melanogaster*	SK_5_9	SMTP	Sweden/VB/Vindelns kommun, Kulbäckslidens försökspark, Gammnybränna/64°08.688′N, 19°35.335′E/01.-22.IX.2003	GU597570	GU597651	GU597812	GU597741
Homotropus nigritarsus	SK_1-F3	NMBE	Switzerland/Graubünden/Sur, Dafora/46°52.470′N, 9°64.591′E/21.-28.VII.2003	FJ556529	GU597652	FJ556462	GU597742
Homotropus nigrolineatus	SK_1-G1	NMBE	Switzerland/Graubünden/Sur, Dafora/46°52.470′N, 9°64.591′E/14.-21.VII.2003	FJ556532	GU597653	FJ556465	GU597743
Homotropus pacificus	SK_1-G7	NMBE	USA/Alaska/Fairbanks, North Star Borough/20.-24.VI.2006	GU597572	GU597656	GU597814	GU597746
Homotropus pallipes	SK_1-G3	NMBE	Finland/Nordösterbotten/Muhos/5.-19.VIII.2005	FJ556533	GU597654	FJ556466	GU597744
Homotropus pictus	SK_1-G4	NMBE	Finland/Southern Finland/Sipoonkorpi/2.-12.VII.2006	GU597571	GU597655	GU597813	GU597745
Homotropus cf. *lissosoma*	SK_5_22	IMUW	Ecuador/Napo Province/Yanayacu biological Station/0°35.9′S, 77°53.4′W/21.-25.VII.2008	GU597551	GU597622	GU597790	GU597712
Homotropus lucidus	SK_2-C10	NMBE	Malaysia/Pahang/Cameron Highlands, Tanah Rata/V.2001	GU597575	GU597662	GU597818	GU597752
Homotropus subopacus	SK_2-B9	NMBE	Finland/Southern Finland/Sipoonkorpi/21.VI.-2.VII.2005	FJ556536	GU597658	FJ556469	GU597748
Homotropus vitreus	SK_6_11	SMTP	Sweden/Vb/Vindelns kommun, Kubäckslidens försökspark, Kulbäcken meadow/64°11.413′N, 19°36.342′E/01.-22.IX.2003	GU597574	GU597661	GU597817	GU597751
Phthorima compressa	SK_1-C9	NMBE	Switzerland/Graubünden/Sur, NE Sur/46°52.419′N, 9°63.425′E/14.VII.-1.VIII.2006	FJ556514	GU597626	FJ556447	GU597716
Phthorima xanthaspis	SK_5_6	SMTP	Sweden/Sö/Tyresö kommun, Ava, Spirudden/59°10.313′N, 18°22.197′E/17.VI.-02.VII.2003	GU597554	GU597627	GU597793	GU597717
Promethes bridgmani	SK_1-C11	NMBE	Finland/Southern Finland/Sipoonkorpi/2.-12.VII.2006	FJ556515	GU597628	FJ556448	GU597718
Promethes melanaspis	SK_4-C2	SMTP	Sweden/An/Ömsköldsviks kommun, Skuleskogen, Langra/63°05.323′N, 18°29.903′E/17.VII.-29.VII.2003	GU597555	GU597629	GU597794	GU597719
Promethes nigriventris	SK_5_7	NMBE	Switzerland/Bern/ Bremgartenwald/46°95.962′N, 7°41.565E/11.-20.VI.2008	GU597556	GU597630	GU597795	GU597720
Promethes sulcator	SK_1-C12	NMBE	Finland/Southern Finland/Sipoon, Hindsby/5.-12.VI.2005	GU597557	GU597631	GU597796	GU597721

Appendix 1 (Continued)

Taxon	Int. code	Collection[a]	Country/Department/Locality/ Coordinates/Collection date	GenBank accession numbers			
				28S D2-3	EF1α	CO1	ND1
Schachticraspedon kropfi	SK_6_5	IMUW	Ecuador/Napo Province/Yanayacu biological Station, Macucoloma trail/0°35.9′S, 77°53.4′W/1.-10.V.2008	GU597549	GU597620	GU597788	GU597710
Sussaba aciculata	SK_1-D3	NMBE	Switzerland/Graubünden/Sur, Dafora/46°52.470′N, 9°64.591′E/16.-23.VI.2003	GU597558	GU597632	GU597797	GU597722
Sussaba cognata	SK_1-D4	NMBE	Switzerland/Bern/Bremgartenwald/ 46°95.962′N, 7°41.565E/4.-15.VIII.2006	GU597559		GU597798	
S. cognata	SK_6_34	NMBE	Switzerland/Bern/Bremgartenwald, Nägelisbode/46°96.592′N, 7°41.761E/23.-30.VII.2008		GU597633		GU597723
Sussaba dorsalis	SK_1-D7	NMBE	Switzerland/Graubünden/Sur, NE Sur/46°52.419′N, 9°63.425′E/1.-25.IX.2006	GU597560		GU597799	
S. dorsalis	SK_6_35	NMBE	Switzerland/Graubünden/Sur, Dafora/46°52.470′N, 9°64.591′E/23.-30.VI.2003		GU597634		GU597724
Sussaba erigator	SK_1-B7	NMBE	Switzerland/Graubünden/Sur, NE Sur/46°52.419′N, 9°63.425′E/15.-27.VII.2006	GU597561	GU597635	GU597800	GU597725
Sussaba flavipes	SK_1-D9	NMBE	Switzerland/Graubünden/Sur, NE Sur/46°52.419′N, 9°63.425′E/14.VII.-1.VIII.2006	GU597562		GU597801	
S. flavipes	SK_6_36	NMBE	Switzerland/Solothurn/Trimbach, Miesernbach/47°36.541′N, 7°87.047′E/13.-21.VI.2002		GU597636		GU597726
Sussaba placita	SK_7_15	IMUW	USA/Wyoming/Yellowstone NP/12.VIII.1990	GU597563	GU597637	GU597802	GU597727
Sussaba pulchella	SK_1-D11	NMBE	Finland/Southern Finland/Sipoon, Hindsby/18.-25.VI.2005	FJ556520		FJ556453	
S. pulchella	SK_6_37	NMBE	Switzerland/Glarus/Linthal, Obersand, Melchplatz/46°83.979′N, 8°9.3035E/10.-19.VII.2008		GU597638		GU597728
Sussaba punctiventris	SK_1-E1	NMBE	Switzerland/Graubünden/Sur, Dafora/46°52.470′N, 9°64.591′E/25.VII.-1.VIII.2003	FJ556521	GU597639	FJ556454	GU597729
Sussaba roberti	SK_1-B9	NMBE	Switzerland/Graubünden/Sur, NE Sur/46°52.419′N, 9°63.425′E/19.-27.VII.2006	GU597564	GU597640	GU597803	GU597730
Sussaba tertia	SK_6_3	IMUW	Ecuador/Napo Province/Yanayacu biological Station/0°35.9′S, 77°53.4′W/2.-4.III.2008	GU597550	GU597621	GU597789	GU597711
Syrphoctonus cf. *borealis*	SK_1-E4	NMBE	USA/Alaska/Fairbanks, North Star Borough/20.-24.VI.2006	GU597576	GU597641	GU597804	GU597731
Syrphoctonus desvignesii	SK_1-E10	NMBE	Switzerland/Graubünden/Sur, NE Sur/46°52.419′N, 9°63.425′E/15.-20.VII.2006	FJ556524	GU597644	FJ556457	GU597734
Syrphoctonus fissorius	SK_1-E11	NMBE	Switzerland/Bern/Bremgartenwald/ 46°95.962′N, 7°41.565E/21.-28.VII.2006	GU597577		GU597808	GU597736
S. fissorius	SK_6_38	NMBE	Switzerland/Glarus/Linthal, Obersand, Melchplatz/46°83.979′N, 8°9.3035E/28.VI.-10.VII.2008		GU597646		
Syrphoctonus idari	SK_5_12	SMTP	Sweden/Vr/Munkfors kommun, Ransäter, Ransbergs herrgard/66°32.516′N, 13°65.816′E/10.VII.-24.VII.2005	GU597578	GU597648	GU597809	GU597738

Appendix 1 (Continued)

Taxon	Int. code	Collection[a]	Country/Department/Locality/ Coordinates/Collection date	GenBank accession numbers			
				28S D2-3	EF1α	CO1	ND1
Syrphoctonus tarsatorius	SK_1-G8	NMBE	Switzerland/Graubünden/Sur, Dafora/46°52.470′N, 9°64.591′E/18.-25.VIII.2003	FJ556537	GU597659	FJ556470	GU597749
S. tarsatorius	SK_6_12	NMBE	Switzerland/Glarus/Linthal, Obersand, Melchplatz/46°83.979′N, 8°9.3035E/28.VI.-10.VII.2008	GU597579	GU597660	GU597816	GU597750
Syrphophilus asperatus	SK_5_14	SMTP	Sweden/Vr/Munkfors kommun, Ransäter, Ransbergs herrgard/66°32.516′N, 13°65.816′E/18.-27.VI.2005	GU597580	GU597663	GU597819	GU597753
Syrphophilus bizonarius	SK_1-G11	NMBE	Turkey/Bolu/Bolu/VI.1999	GU597581	GU597664	GU597820	GU597754
Syrphophilus tricinctorius	SK_1-G12	NMBE	Switzerland/Graubünden/Sur, Claveina/46°52.037′N, 9°65.645′E/2.-9.VI.2003	GU597582	GU597665	GU597821	GU597755
S. tricinctorius	SK_1-H1	NMBE	Finland/Southern Finland/Sipoonkorpi/16.-21.VI.2006	GU597583	GU597666	GU597822	GU597756
Syrphophilus tricinctus	SK_5_15	SMTP	Sweden/Hr,/Härejdalens kommun, Sanfjället, Nyvallens fäbod/62°19.001′N, 13°34.113′E/04.VII.-04.VIII.2004	GU597584	GU597667	GU597823	GU597757
Tymmophorus erythrozonus	SK_1-B10	NMBE	Switzerland/Graubünden/Sur, Dafora/46°52.470′N, 9°64.591′E/30.VI.-7.VII.2003	FJ556541	GU597668	FJ556474	GU597759
T. erythrozonus	SK_1-B11	NMBE	Switzerland/Graubünden/Sur, NE Sur/46°52.419′N, 9°63.425′E/14.VII.-1.VIII.2006	FJ556542	GU597669	FJ556475	GU597760
Tymmophorus obscuripes	SK_1-H2	NMBE	England, ?	FJ556543	GU597670	FJ556476	GU597758
Tymmophorus suspiciosus	SK_2-B11	NMBE	Finland/Nordösterbotten/Muhos/5.-19.VIII.2005	FJ556545	GU597671	FJ556478	GU597761
Woldstedtius bauri	SK_4-F12	SMTP	Sweden/Ög/Ödeshögs kommun, Omberg, Storpissan/58°20.095′N, 14°39.300′E/28.V.-5.VII.2005	GU597588	GU597678	GU597827	GU597768
Woldstedtius biguttatus	SK_1-H4	NMBE	England, ?	GU597585	GU597672	GU597824	GU597762
W. cf. *biguttatus*	SK_2-B12	NMBE	Korea/Gangwon-do/Goseong, Ganseong, Heulri (Shinseonbong)/2.VIII.-19.X.2002	GU597586	GU597675	GU597826	GU597765
Woldstedtius citropectoralis	SK_2-C4	NMBE	Finland/Nordösterbotten/Muhos/5.-19.VIII.2005	FJ556548	GU597673	FJ556481	GU597763
Woldstedtius flavicauda	SK_1-H12	NMBE	Chile/XI.2001	GU597589	GU597679	GU597828	GU597769
Woldstedtius flavolineatus	SK_1-H8	NMBE	Switzerland/Graubünden/Sur, Claveina/46°52.037′N, 9°65.645′E/23.-30.VI.2003	GU597587	GU597674	GU597825	GU597764
Woldstedtius holarcticus	SK_1-H10	NMBE	Switzerland/Bern/Bremgartenwald/ 46°95.962′N, 7°41.565E/21.-28.VII.2006	FJ556550	GU597676	FJ556483	GU597766
W. holarcticus	SK_1-H11	NMBE	Finland/Southern Finland/Sipoonkorpi/21.VI.-2.VII.2005	FJ556551	GU597677	FJ556484	GU597767
Woldstedtius isidroi	SK_6_4	IMUW	Ecuador/Napo Province/Yanayacu biological Station/0°35.9′S, 77°53.4′W/21.-25.VII.2008	GU597552	GU597623	GU597791	GU597713
Xestopelta gracilima	SK_3-C3	NMBE	England/Merseyside/Hilbre Island/53°35.702′N, 3°07.574′W/21.VII.2001	GU597590		GU597829	GU597770
X. gracilima	SK_4-E12	SMTP	Sweden/Sö/Tyresö kommun, Ava, Spirudden/59°10.313′N, 18°22.197′E/12.-28.V.2004		GU597680		

Appendix 1 (Continued)

Taxon	Int. code	Collection[a]	Country/Department/Locality/ Coordinates/Collection date	GenBank accession numbers			
				28S D2-3	EF1α	CO1	ND1
Collyriinae							
Collyria trichophthalma	SK_5_16	NMBE	Switzerland/Luzern/Luzern, Allmend/47°03′N, 8°18′E/10.VI.2006	GU597593	GU597683	GU597832	GU597773
Cylloceriinae							
Cylloceria cf. *melancholica*	SK_1-F7	NMBE	Finland/Nordösterbotten/Muhos/5.-19.VIII.2005	GU597594	GU597684	GU597833	GU597774
Orthocentrinae							
Entypoma sp.	SK_1-F11	NMBE	Finland/Nordösterbotten/Muhos/5.-19.VIII.2005	GU597596	GU597686	GU597835	GU597776
Picrostigeus cf. *obscurus*	SK_1-F10	NMBE	Finland/Nordösterbotten/Muhos/5.-19.VIII.2005	GU597595	GU597685	GU597834	GU597775
Pimplinae							
Apechthis quadridentata	SK_1-F8	NMBE	Finland/Nordösterbotten/Muhos/5.-19.VIII.2005	GU597592	GU597682	GU597831	GU597772
Rhyssinae							
Rhyssa amoena	SK_2-A2	NMBE	Finland/Southern Finland/Sipoonkorpi/23.VI.-3.VII.2006	GU597597	GU597687	GU597836	GU597777
Ichneumoninae							
Ichneumon cf. *minutorius*	SK_6_8	NMBE	France/Hautes-Alpes/Col du Lautaret/45°20′N, 6°24′E/2008	GU597591	GU597681	GU597830	GU597771

[a]Collection: the vouchers are stored in the following collections.

NMBE, Natural History Museum, Bern, Switzerland; SMTP, Swedish Malaise Trap Project, Öland, Sweden; Insect Museum, University of Wyoming, Laramie, USA.

Appendix 2 Morphological characters scored for phylogenetic analysis

No.	Character with states	Steps	CI	RI	Figure
1	Tyloids (release and spread structures) on the antennae of males: (0) absent; (1) present.	6	0.17	0.84	1A–D
2	Shape of tyloids: (?) tyloids absent; (1) linear, very narrow; (2) drop-shaped, apically more narrow than towards basal part of the antennal segment; (3) linear, very broad; (4) oval; (5) deep concavity on basal part of segment	4	1.00	1.00	1A–D
3	Length of tyloids: (?) tyloids absent; (1) shorter than antennal segment; (2) as long as antennal segment	3	0.33	0.80	1A–D
4	Colour of tyloids: (?) tyloids absent; (0) uniformly brown; (1) two-coloured, with light area ventrally and dark brown area dorsally	1	1.00	1.00	
5	Location of tyloids: (?) tyloids absent; (1) on median antennal segments; (2) apical, from middle to close to apex; (3) basal, from antennomeres 4 to about middle; (4) on antennomeres 3 and 4	6	0.50	0.82	
6	Courtship behaviour: (0) not performing antennal coiling; (1) performing antennal coiling (Klopfstein *et al.* 2010b)	4	0.25	0.90	
7	Type of antennal courtship: (?) coiling behaviour absent; (1) single coiling; (2) double coiling; (3) bend (Klopfstein *et al.* 2010b)	4	0.50	0.85	
8	Sensillae on ventral area of apical antennal segments: (0) as dorsally, multiporous plate sensillae and hair-like sensillae uniformly distributed; (1) devoid of multiporous plate sensillae, without cone sensillae; (2) without multiporous plate sensillae, but with dense cone-like sensillae	7	0.29	0.50	1E–F
9	Colour of the antenna: (0) brown or black; (1) bright orange	6	0.17	0.00	
10	Length of antenna: (0) short, with <20 segments; (1) intermediate, 20–22 segments; (2) long, more than 22 segments	20	0.10	0.51	

Appendix 2 (Continued)

No.	Character with states	Steps	CI	RI	Figure
11	Length of shortest antennal segments: (0) quadratic; (1) 1.1–1.25 times longer than wide; (2) more than 1.3 times longer than wide	25	0.08	0.44	
12	Vertical grooves above clypeus: (0) absent; (1) present	3	0.33	0.80	1G–I
13	Number of teeth of mandible: (0) two teeth; (1) three teeth (upper tooth subdivided into two teeth)	1	1.00	1.00	1G–I
14	Punctuation of the face: (0) absent or weak; (1) present and distinct	18	0.06	0.39	
15	Background sculpture of the face: (0) smooth and shining; (1) coriaceous, matt	6	0.17	0.67	1G–I
16	Groove between compound eye and mandible: (0) absent; (1) indicated as a change in sculpture on part of the length; (2) distinct groove on whole length	12	0.17	0.38	
17	Apical margin of clypeus: (1) thin; (2) thick, thus clypeus protruding apically	2	0.50	0.50	1G–I
18	Shape of clypeus: (0) with a deep median notch, rendering the clypeus bi-lobate; (1) with apical margin straight or at most weakly excised	13	0.08	0.64	1G–I
19	Profile of clypeus: (0) convex on basal third, remainder concave or flat; (1) convex on basal two-thirds, apical margin impressed; (2) all convex	7	0.29	0.76	1G–I
20	Yellow eye margins of female: (0) absent; (1) present	4	0.25	0.88	
21	Yellow colouration face female: (0) absent; (1) with a central facial spot; (2) face all yellow	14	0.14	0.63	
22	Yellow eye margins of male: (0) absent; (1) present	1	1.00	1.00	
23	Yellow colouration face male: (0) absent; (1) with a central facial spot; (2) face all yellow	10	0.20	0.20	
24	Areolet cell in forewing: (0) absent (open); (1) closed, but outer nerve only partly pigmented; (2) closed with strong, fully pigmented nerve	10	0.20	0.56	
25	Number of costal hamuli on hind wing: (1) one; (2) two or more	3	0.33	0.88	
26	Prepectral carina: (0) reduced ventrally; (1) fully developed	7	0.14	0.40	
27	Punctuation of mesonotum: (0) with indistinct punctures; (1) with distinct punctuation on whole surface	18	0.06	0.48	
28	Sculpture of mesonotum: (0) smooth and shining; (1) coriaceous and matt	10	0.10	0.59	
29	Punctuation of mesopleuron: (0) with indistinct punctures; (1) with distinct punctuation on whole surface	19	0.05	0.51	
30	Sculpture of mesopleuron: (0) smooth and shining; (1) coriaceous and matt	11	0.09	0.62	
31	Notauli on mesonotum: (0) absent; (1) short but distinct, present as a groove only on declivity; (2) reaching on dorsal surface of mesonotum; (3) reaching over most of mesonotum	7	0.43	0.85	
32	Lateral ridges of scutellum: (0) only reaching over prescutellar ridge; (1) reaching to at least half the length of the scutellum	3	0.33	0.85	
33	Yellow shouldermarks: (0) absent; (1) present as spots; (2) present as long bars with the median corner extended onto mesonotum	19	0.11	0.48	
34	Colour of scutellum: (0) all black; (1) yellow on sides or hind margin; (2) all yellow; (3) red	25	0.12	0.37	
35	Shape of propodeum: (0) rounded; (1) strongly shortened; (2) elongated	4	0.50	0.60	
36	Carination of propodeum: (1) with full set of carinae delimiting basal, apical and lateral areas; (2) carinae partly reduced, but at least one transverse carina present; (3) only metapleural carina present; (4) carinae fully reduced	16	0.19	0.61	1J–L
37	Sculpture of the petiolar area: (0) smooth and shining; (1) shagreened; (2) carinulate	16	0.13	0.66	1J–L
38	Ventral carina of metapleuron: (0) present as a normal carina; (1) extended into a small flange; (2) forming a large flange that overlaps the mid coxae	17	0.12	0.50	
39	Shape of metasoma: (0) dorsoventrally depressed; (1) basally depressed, but compressed apically, thus tapered from base to apex; (2) very strongly compressed from third segment, knifelike	22	0.09	0.26	
40	Colouration of metasoma: (0) all black; (1) with red on median tergites; (2) with yellow hind margins on tergites 2–5; (3) with yellow triangles on each tergite	20	0.15	0.39	
41	Transverse impression on tergites: (0) absent; (1) indicated on one or two tergites; (2) distinct on at least three tergites	4	0.50	0.91	1M–N

Appendix 2 (Continued)

No.	Character with states	Steps	CI	RI	Figure
42	Shape of hind margin of tergites: (0) convex or straight; (1) slightly concave on tergites 5 and 6; (2) strongly concave from tergite 3 or 4 to apex	7	0.29	0.29	
43	Dorsal carinae on first tergite: (0) absent or weak; (1) distinct, broadly separated from each other; (2) present, converging and very close to each other on apical part of tergite	9	0.22	0.70	1M–N
44	Sculpture of first tergite: (0) without striae; (1) striate or carinulate on lateral parts	11	0.09	0.52	
45	Lateral ridge and groove on second tergite (glymna): (0) absent; (1) only ridge present, without groove; (2) both ridge and groove present	18	0.11	0.66	
46	Dorsal carinae on second tergite: (0) absent; (1) present as two distinct ridges	1	1.00	1.00	
47	Carina between base and spiracle of third tergite: (0) absent; (1) present	5	0.20	0.43	
48	Position of spiracle of the second tergite: (1) on dorsal part of tergite; (2) on laterotergite, below the crease separating it from the dorsal part	1	1.00	1.00	
49	Position of spiracle of the third tergite: (1) on dorsal part of tergite; (2) behind the crease, about level with it; (3) on laterotergite, clearly below the crease separating it from the dorsal part	13	0.15	0.52	
50	Punctuation of second tergite: (0) absent; (1) distinctly punctured	10	0.10	0.40	
51	Sculpture of second tergite: (0) smooth and shining; (1) coriaceous and matt; (2) carinulate	15	0.13	0.65	
52	Longitudinal striae on second tergite: (0) restricted to basal 0.2; (1) reaching to the middle of the tergite	11	0.09	0.47	
53	Sternites 3 and 4 of the female: (0) with lateral and median part sclerotized; (1) with median part reduced to a membraneous area	8	0.13	0.50	
54	Sternite 5 of the female: (0) with lateral and ventral parts completely separated; (1) fused from behind middle to a synsternum; (2) completely fused to a synsternum; (3) separate along mid-axis (median part reduced)	26	0.12	0.38	
55	Sculpture of hind coxa: (0) smooth (except for hair roots); (1) coriaceous	14	0.07	0.62	
56	Length of hind tibial spurs: (0) shorter than 0.4 times hindtarsus 1; (1) distinctly longer than 0.5 times hindtarsus 1	2	0.50	0.83	
57	Scale-like hairs on outer surface of hind tibia: (0) absent; (1) present	12	0.08	0.45	
58	Colour of coxae: (0) mainly black; (1) mainly red or yellow	20	0.05	0.46	
59	Colour pattern of hind femora: (0) all black or with black stripe; (1) black with a median light band; (2) red	6	0.33	0.00	
60	Colouration of hind tibia: (1) black with a white base; (2) white with the apex and a subbasal spot black; (3) black with a median white band; (4) red or orange	12	0.25	0.71	
61	Tip of ovipositor sheats: (0) closed; (1) diagonally truncate, thus open at tip; (2) transversely truncate	9	0.22	0.65	1O–P
62	Shape of ovipositor sheats: (0) very stout, compressed, section close to the end circular; (1) stout, not compressed, section close to the end circular; (2) stout, laterally compressed, sides parallel; (3) stout, laterally compressed, sides not parallel, with widest part in apical third; (4) slender, long, laterally compressed and upcurved; (5) very long, transversely striate; (6) continuously tappered from base to apex	18	0.39	0.76	1O–P
63	Tergites 9 and 10 of the male: (0) fused as a syntergum; (1) as distinct sclerites; (2) fused, but tergite 10 separated into two parts	3	0.67	0.96	2A–C
64	Shape of sternite 9 of the male: (0) uni-lobate; (1) bi-lobate; (2) with bilobate part, but upper triangle present as membraneous area	5	0.40	0.80	2D–F
65	Proportions of sternite 9: (0) higher than wide; (1) at most 1.5 times wider than high; (2) more than 2 times wider than high, and with lobes very deeply excised	8	0.25	0.83	2D–F
66	Outer corners of sternites 9: (0) rounded; (1) bluntly angulate; (2) with an acute angle (<85°)	7	0.29	0.58	2D–F

Steps, number of steps on the total evidence phylogeny; CI, consistency index; RI, retention index; Fig., reference to figure if available.

Appendix 3 Partitioning strategies, associated log likelihoods and Bayes factors

Strategy	#part	Specification	ln *L*	Bayes factor
P1	1	Unpartitioned dataset	−29560.2	4299
P2a	2	Partitioned into third codon positions (of CO1, ND1, EF1α) and remainder	−28909.2	2997
P2b	2	Partitioned into mtDNA (CO1, ND1) vs. nuclear DNA (28S, EF1α)	−28948.6	3076
P2c	2	Partitioned into ribosomal RNA (28S) vs. protein-coding genes (CO1, ND1, EF1α)	−29270.7	3720
P4	4	Partitioned into the four genes	−28410.1	1999
P6	6	Partitioned into stems and loops of 28S, first + second vs. third codon positions of EF1α, and first + second vs. third codon positions of the combined mtDNA genes (CO1, ND1)	−27997.6	1174
P8a	8	Partitioned into stems and loops of 28S, and into first + second vs. third of each protein coding gene (CO1, ND1, EF1α)	−27643.9	467
P8b	8	Partitioned as under P8, and doublet model for the pairing stem partition of 28S	−27410.7	–

#part, number of partitions; ln *L*, harmonic mean of the log likelihoods obtained under the respective partitioning strategy; Bayes factor, Bayes factor calculated from the comparisons with the best-fitting partitioning strategy P8b; EF1a, elongation factor 1α.

Appendix 4 Definitions of the genera Fossatyloides, Homotropus and Syrphoctonus

Fossatyloides gen. n.

Type species. *Bassus gracilentus* Holmgren, 1858

Etymology. The name *Fossatyloides* refers to the peculiar structures found on the antennae of the males. Beside the linear, narrow tyloids as they are common in the genus group (cf. Fig. 1A), the males of this genus have circular holes.

Diagnosis. This genus has unique modifications of the antennae in the male sex, with a hole adjacent to the linear, narrow tyloid which is the rule in the genus group. The petiolar area of the propodeum is enclosed by several parallel carinae, another distinctive feature.

Description. 4.9–5.6 mm. Face coriaceous and matt, without vertical impressions, in the female all black, in the male all yellow. Clypeus with apical margin thin, impressed along the margin, resulting in the central area being convex. Antenna long, with 19–21 flagellomeres, last flagellomeres much longer than wide, in the males with linear, narrow tyloids and adjacent holes, without long setae. Mesonotum with notauli indistinct; all smooth and shining, yellow shouldermarks large, their inner corners usually extended into two parallel lines on mesonotum; mesopleuron with some irregular sculpture on lower part; epicnemial carina complete ventrally. Propodeum with longitudinal carinae present, but basal area only indicated by weak carinae, with petiolar enclosed by several concentric, arcuate carinae; propodeal spiracle inconspicuous; scutellum not carinate. Areolet in forewing present, but outer vein often without pigmentation; hindwing with two basal hamuli. Hind tibia orange. Metasoma of the female evenly tapered from fourth segment to apex, posterior margins of the tergites convex, tergites without transverse impressions. First tergite without dorsal carinae. Second and third tergite with spiracle dorsally, above the crease separating it from the laterotergite. Metasoma black, marked with orange on tergites 2–4 or 5. Ovipositor sheats 0.3 times as long as hind tibia, tapered and diagonally truncated at apex, thus with the extreme tip of the ovipositor exposed; with inconspicuous hairs ventrally and at apex. Male with tergites 9 and 10 as distinct sclerites, sternite 9 about two times wider than long, emarginated apically, thus forming two lobes, their outer corners rounded.

Species in this genus. There is currently only the type species included in this genus. According to the description (Dasch, 1994), the Nearctic *Homotropus sicarius* Dasch also belongs to this genus, a placement that we would like to assure in the future.

Homotropus Förster, 1869

Type species. *Bassus elegans* Gravenhorst, 1829

Diagnosis. In most *Homotropus* species, the clypeus is impressed along the apical margin, making it convex when viewed from the side. The epicnemical carina is always complete. These features are only shared with *Fossatyloides* and *Phthorima*. From the first, *Homotropus* can be distinguished by the convex apical margins of the tergites and the mostly coriaceous and matt face. From Fossatyloides, it can be separated by the lack of holes adjacent to the tyloids on the antennae of the male, and by the lack of parallel carinae around the petiolar area. The exact limits of this genus, however, require additional investigation, and a more profound diagnosis should await the inclusion of additional species groups into a phylogenetic analysis.

Description. Face coriaceous and matt, without vertical impressions, in the female all black or black with a yellow central patch, in the male all yellow or black with yellow inner eye margins and a yellow central patch. Clypeus usually with apical margin thin, impressed along the margin, resulting in the central area being convex. Antenna long, last flagellomeres usually longer than wide, in the males with linear, narrow tyloids, without long setae.

Mesonotum with notauli indistinct; sculpture various, ranging from all smooth and shining, with or without punctures to being

strongly coriaceous and matt, yellow shouldermarks present or absent, their inner corners sometimes extended into two parallel lines on mesonotum; mesopleuron sometimes all smooth and shining, but often with punctures and/or coriaceous sculpture at least on the lower half; epicnemial carina complete ventrally. Propodeum various, sometimes with a full set of carinae enclosing basal, petiolar and lateral areas, but usually with carinae partly or fully reduced; propodeal spiracle inconspicuous; scutellum not carinate. Areolet in forewing sometimes absent, but usually present, but outer vein often without pigmentation; hindwing with 2–4 basal hamuli. Hind tibia various, orange, yellow or white with a dark apex and subbasal spot. Metasoma of the female usually evenly tapered to apex, but sometimes strongly compressed from behind third segment, but never with posterior margins of the tergites concave; tergites without transverse impressions. First tergite usually without dorsal carinae, but if present, they are converging on basal half and are parallel and widely separate on apical half. Second tergite with spiracle dorsally, above the crease separating it from the laterotergite, third tergite with spiracle usually above, but rarely below or behind the crease. Metasoma black, sometimes with yellow markings, or marked with red. Ovipositor sheats 0.3 times as long as hind tibia, either parallel-sided and fully enclosing ovipositor or tapered and diagonally truncated; with inconspicuous hairs ventrally and at apex. Males with tergites 9 and 10 as distinct sclerites, sternite 9 about two times wider than long, emarginated apically, thus forming two lobes, their outer corners rounded.

Species in this genus. This genus name was long used for the genus later named *Syrphoctonus*. After the present revalidation of *Homotropus* as a separate genus, many of the previous combinations thus become valid again. We have included the following species in this genus: *Homotropus crassicornis* Thomson, *Homotropus crassicrus* Thomson, *Homotropus elegans* (Gravenhorst), *Homotropus longiventris* Thomson, *Homotropus melanogaster* (Holmgren), *Homotropus nigritarsus* (Gravenhorst), *Homotropus nigrolineatus* Strobl, *Homotropus pallipes* (Gravenhorst), *Homotropus pictus* (Gravenhorst), *Homotropus signatus* (Gravenhorst), *Homotropus subopacus* (Stelfox), and *Homotropus vitreus* Dasch. Many more of the species previously included in *Syrphoctonus* but not covered in this analysis will probably be moved to *Homotropus* in the future.

Syrphoctonus Förster, 1869

Type species. Bassus exsultans Gravenhorst, 1829

Diagnosis. This genus can be separated from the former by the position of the spiracle of the third tergite below or behind the crease separating the lateral from the dorsal part, by the epicnemical carina which is interrupted behind the front coxae, and by the shape of the clypeus which is impressed along the margin only laterally, with the central area flat or even concave.

Description. Face coriaceous and matt, without vertical impressions, in the female all black or black with a yellow central patch, in the male all yellow. Clypeus with apical margin thin, with a basal thickening and impressed only on the sides, resulting in the central area being convex and the sides being concave. Antenna long, last flagellomeres longer than wide, in the male with linear, narrow tyloids, without long setae. Mesonotum with notauli indistinct; coriaceous and matt with inconspicuous, but sometimes dense punctures; yellow shouldermarks usually present; mesopleuron either all coriaceous and matt or more smooth especially on the upper half, never with strong punctures; epicnemial carina interrupted behind the fore coxae. Propodeum with carinae reduced, at most with some traces of lateral carinae; propodeal spiracle inconspicuous; scutellum not carinate. Areolet in forewing absent, although very rarely present as an aberration in *Syrphoctonus tarsatorius*; hindwing with 2–3 basal hamuli. Hind tibia white, yellow or red with apex infuscate. Metasoma of the female evenly tapered to apex; tergites without transverse impressions. First tergite without dorsal carinae. Second tergite with spiracle dorsally, above the crease separating it from the laterotergite, third tergite with spiracle below or behind the crease. Metasoma black, often with yellow apical bands on most tergites, or orange on median tergites. Ovipositor sheats 0.3 times as long as hind tibia, rather stout, laterally compressed, slightly tapered and fully enclosing ovipositor or diagonally truncate, with inconspicuous hairs ventrally and at apex. Males with tergites 9 and 10 as distinct sclerites, sternite 9 about two times wider than long, emarginated apically, thus forming two lobes, their outer corners rounded.

Species in this genus. This genus should probably be restricted to the *fissorius* and *tarsatorius* species groups as defined by Dasch (1994). Certainly included are the following species which we covered in the present analysis: *Syrphoctonus desvignesii* (Marshall), *Syrphoctonus fissorius* (Gravenhorst), *Syrphoctonus idari* Diller and *Syrphoctonus tarsatorius* (Panzer).

Supporting Information

Additional Supporting Information may be found in the online version of this article:

The molecular and morphological data and the resulting trees are provided as supporting information.

Please note: Wiley-Blackwell are not responsible for the content or functionality of any supporting materials supplied by the authors. Any queries (other than missing material) should be directed to the corresponding author for the article.